UNIVERSITY OF CALIFORNIA, SAN DIEGO

Hydrosilylation of Imines Using a Ni(0) Catalyst

A Thesis submitted in partial satisfaction of the requirements for the degree Masters of Science

in

Chemistry

by

Daniel Patrick Spence

Committee in charge:

Professor Joshua Figueroa, Chair
Professor Joseph O'Connor
Professor Charles Perrin

The Thesis of Daniel Patrick Spence is approved, and it is acceptable in quality and form for publication on microfilm and electronically:

Chair

University of California, San Diego

2016

DEDICATION

Dedicated to my son Liam Jaxon Spence.

TABLE OF CONTENTS

LIST OF FIGURES

LIST OF SCHEMES

ACKNOWLEDGMENTS

There are many people to thank along my journey as a graduate student. First and foremost, I would like to thank my wife who has been very supportive of my endeavors to become a better scientist through this program. With the birth of my first child shortly after beginning my graduate studies, it truly was difficult. My wife made the sacrifice by taking care of our household on nights I was working late and never lost support of me the entire way. Thank you again. This could have never been possible without someone like you.

I would like to thank my advisor Joshua Figueroa, who understood my situation of being a full time employee/part-time student and was very accommodating within his research group to include me. Our meetings and talks have truly been enlightening and have directed me in a path to becoming a better scientist. Thank you for your thought provoking insight and ideas you continually bring to the table.

Last but not least, the members of my group have been instrumental in my learning success as a graduate student. I would especially like to thank Charles Mokhtarzadeh for his patience in teaching me the complexities of solving crystal structures and showing me the ropes in synthesizing isocyanide ligand. He has always found the time out of his busy schedule to help me and others within our group, and I truly thank you for that. I would also like to thank Kyle Mandla who I first spoke with during a poster session and whose research was a key factor in me wanting to join the Figueroa group. Thanks to all others in my group who are such brilliant people and will (or already have) made an impact in chemistry.

ABSTRACT OF THE THESIS

Hydrosilylation of Imines Using a Ni(0) Catalyst

By

Daniel Patrick Spence

Masters of Science in Chemistry

University of California, San Diego, 2016

Professor Joshua S. Figueroa, Chair

The following herein introduces a Ni(0) catalyst that effectively does hydrosilylation of imines to form the corresponding aminosilanes which are of interest in the electronics industry. Preliminary studies of bis-1,5-cyclooctadienyl nickel(0), $Ni(COD)_2$, showed it to be an effective catalyst with relatively good conversion at room temperature and low catalyst loadings (~3%). However, selectively for the aminosilane was limited since there was a significant amount of conversion to the corresponding amine. To circumvent amine production, a combination of using a reengineered Ni(0) catalyst and a new silane was used. $Ni(COD)_2$ was reacted with two equivalents of the sterically encumbering *m*-terphenyl isocyanide $CNAr^{Mes2}$ (Ar^{Mes2} = 2,6-(2,4,6-$Me_3C_6H_2)_2C_6H_3$) to form $Ni(COD)(CNAr^{Mes2})_2$. In turn, it was used in the catalyst studies showing

less propensity to dehydrocouple and a better selectively for the desired aminosilane. Using hexylsilane in place of phenylsilane led to further improvement, showing complete selectivity for the aminosilane. A scope of imines was explored and showed rather consistent reaction rates (t = 2hr) at room temperature at low catalyst loading (3-2.5%). Studies were carried out to try and isolate an intermediate in the catalytic cycle where oxidative addition occurs of $Ni(COD)(CNAr^{Mes2})_2$ with the silane. Insight is given into the possible mechanism.

Introduction

Aminosilanes are important as precursors in the production of microelectronics. Their delivery via ALD or CVD processes makes it necessary that they have a relatively high vapor pressure as well as thermal stability. They can be delivered to provide a number of different films spanning silicon oxide, silicon carbide, silicon nitride and mixtures of the three in order to provide electrical and mechanical properties needed for the film.

Of particular value is an aminosilane's ability to anchor via their amino group on a surface thus liberating amine that can be easily removed under reduced pressure. Due to the cost of amines and the laborious work needed in synthesizing aminosilanes via amination of a chlorosilane, it is of particular interest if one could gain access to aminosilanes using imines via hydrosilylation. Imines are relatively straight forward to synthesize via condensation of a ketone with a primary amine. Of added importance is the use of catalysts composed of abundant metals such as iron, cobalt, and nickel rather than more expensive rare metals such as ruthenium, palladium, or platinum. Literature exists of hydrosilylation of imines spanning a range of metal catalysts such as Zn[1], Fe[2, 3], Ru[4-7], Rh[8, 9], Ir[10-12], and Pd[13]. Herein is described the hydrosilylation of a variety of imines to aminosilanes using Ni(0) catalysts.

Groundwork

The goal of this project was to find a novel metal-ligand system that does hydrosilylation of imines. The first step required synthesis and purification of an imine that would be used in screening potential catalysts in the presence of phenylsilane. The synthesis of 4-methyl-N-(1-phenylethylidene)-benzenamine (**imine-1**) was successfully done and was characterized by GC-MS and [H^1]NMR. Efforts were then focused on screening group 8, 9, and 10 metal complexes at 2-5 mol% loading. Some complexes (e.g. $[RhCODCl]_2$, $[IrCODCl]_2$, and Wilkison's catalyst) gave interesting results in that they did a degree of hydrogenation of the imine to form the corresponding amine. Reactions were monitored first on a weekly time scale, then on a 24-hour time scale by GC-MS. Of all the group 8, 9, and 10 complexes screened, $Ni(COD)_2$ formed evidence of the desired monoaminosilane. Due to this observation, we wanted to focus our efforts in reproducing this result by repeating the reaction. The catalysis of $Ni(COD)_2$ at 3-4 mol% loading showed reproducibility.

The next step involved optimizing the formation of the desired aminosilane with $Ni(COD)_2$ by changing the amount of reactants used, order in which each reactant was delivered, as well as the reaction temperature. It was found that increasing the catalyst loading mol%, increasing the amount of phenylsilane, and increasing the temperature (70°C) all contributed modestly in the formation of the desired aminosilane. The order in which the reactants were delivered did not make a difference. We then wanted to better understand the hydrosilylation reaction mechanism involved with $Ni(COD)_2$ to gain insight into optimizing the formation of the desired monoaminosilane. In order to do this, a stoichiometric amount of $Ni[COD]_2$ was reacted with phenylsilane to see what intermediate complex might be formed *in situ* during catalysis. It was proposed that a η-6 Ni-Ph or a μ-3 agostic Ni-H-Si interaction may exist. In another respect,

in situ formation of Ni(0) complexes from $Ni[COD]_2$ and the substitution of phosphines (e.g triphenylphosphine and tricyclohexylphosphine) did not provide any advantage over the $Ni[COD]_2$ system. Understanding the mechanism associated with hydrosilylation was important, so understanding the interaction of all components through analytical tools as well as isolation and characterization of intermediates was essential.

Initial Studies

A sound understanding of prior art was essential in achieving a novel metal-ligand system in the hydrosilylation of imines. Alexander H. Vetter and Albrecht Berkessel report a catalyst formed by the 1:1 addition of [Ni(OAc)2] and O,N,S pincer type ligands that does hydrosilation of imines[14]. Bheeter *et al* report a Ni(II) NHC pre-catalyst that in the presence of $NaHBEt_3$ forms the active Ni-H species which can catalyze the reduction of a large scope of aldimines and ketamines using Ph_2SiH_2. They also report a cationic analogue which does the same[15].

With respect to the following prior art, hydrosilylation of imines using a nickel catalyst is rare. Furthermore, there seems to be no prior literature for a Ni(0) catalyst that does hydrosilylation of imines. The goal of the previous literature was to hydrosilylate via the aminosilane intermediate, then isolate the desired amine by cleaving under acidic conditions. In contrast, the goal of our study was to isolate the aminosilane which is of interest in the electronics industry as precursors for ALD/CVD[16, 17].

The following structural template for imines was used for the hydrosilylation studies:

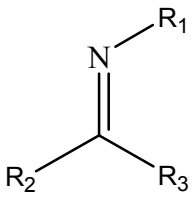

The following catalysts were used:

1 = 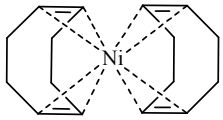

2 = 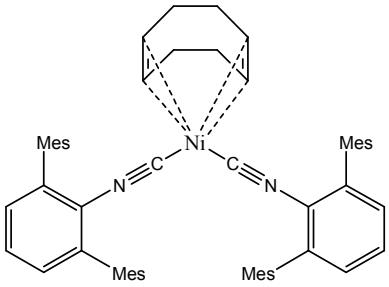

To a solution of **1** (3% molar loading) in deuteriated benzene was added **imine-1**, followed by two equivalents of phenylsilane (Scheme 1). Over the course of a week at room temperature, [H^1]NMR showed a molar ratio of the corresponding aminosilane to amine of 3:2. The aminosilane can be distinguished from the amine by a quartet at 4.76ppm. The amine splits as a quintet at 4.23ppm due to the adjacent methyl and splitting of the additional N-H. A similar reaction was performed by altering the R_2 from phenyl to a methyl group in 4-methyl-N-(1-methylethylidene)-benzenamine (**imine-2**) and after two hours, [H^1]NMR showed a molar ratio of the corresponding aminosilane to amine of 1:2. The aminosilane can be distinguished from the amine by a septet at 3.67ppm. The amine splits as an octet at 3.34ppm due to the two adjacent methyl and the splitting of the additional N-H. Although the rate of reaction was enhanced with **imine-2**, selectivity for the aminosilane suffered.

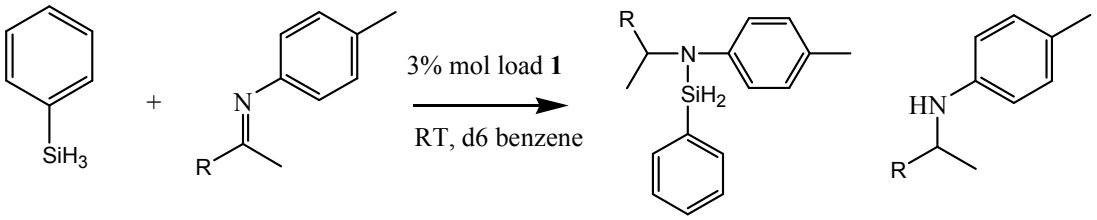

Scheme 1. Preliminary hydrosilylation experiment.

Although the $Ni(COD)_2$ system did well with respect to catalyst loadings and rates, the cons seem to outweigh the pros. First and foremost, $Ni(COD)_2$ is unstable at room temperature and decomposes to nickel metal and 1,5-cyclooctadiene. Secondly, after catalysis, a significant amount of amine is formed.

Next, it was of interest to determine the order of aminosilane/amine evolution. A [H^1]NMR study was performed of the **imine-1**/phenylsilane system and monitored in one hour increments. The evolution of aminosilane was witnessed first, followed by evolution of amine after 16 hours (Figure 1). It was proposed that the evolution of H_2 may enter the catalytic cycle and likewise produce the amine via a reductive elimination step.

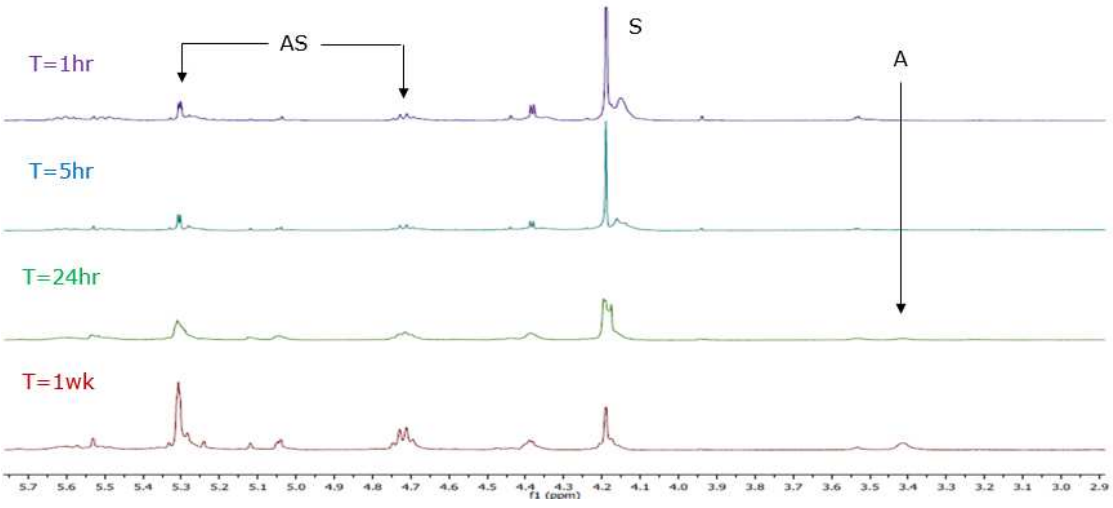

Figure 1. Proton NMR progression of hydrosilylation over one week.

The possibility also exists that once the aminosilane is generated, the active catalyst could be participating in a separate catalytic cycle and cleaving the Si-N bond to form free amine. To put this later theory to practice, a control was set up using a purified primary aminosilane ($(iPr)_2NSiH_3$) in the presence of **2**. Over the course of 16 hours monitored by GC-MS,

there seemed to be no further evolution of amine than that already contained in the sample. It is still unclear why amine is generated, even in a moisture free environment.

Sterically encumbering m-terphenyl isocyanide ligands have been shown to stabilize coordinatively unsaturated metal complexes[18-22]. More specifically, 2'-isocyano-2,2'',4,4'',6,6''-hexamethyl-1,1':3',1''-terphenyl, or DMP, coordinates to nickel to provide some complexes of interest[18]. Ligands that stabilize the metal center via a synergy of σ-bonding/∏-back-bonding such as isocyanides can be utilized to provide a stable Ni(0) structure that can have potential as a hydrosilylation catalyst. Two equivalents of the isocyanide (DMP) were added to **1** in diethyl ether at room temperature to form **2** in 73% yield as a vibrant orange complex was used in the same catalyst studies as $Ni(COD)_2$ (Scheme 2).

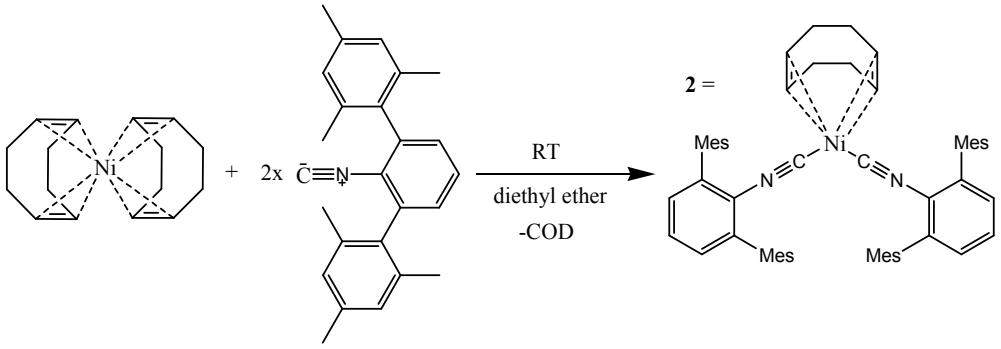

Scheme 2. Reaction scheme for synthesis of NiCOD(DMP)2.

To a solution of **2** (3% molar loading) in deuterated benzene was added **imine-1** followed by two equivalents of phenylsilane (Scheme 3).

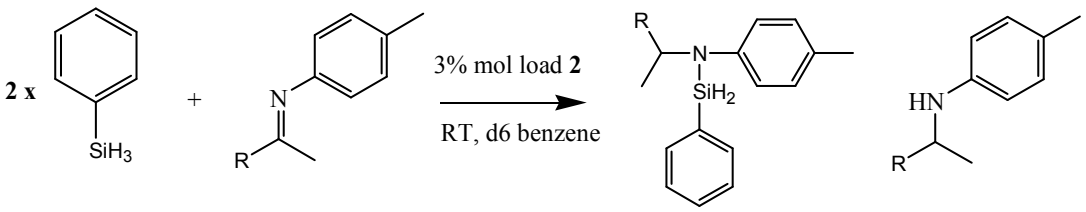

Scheme 3. Secondary hydrosilylation experiment.

Over the course of a week at room temperature, [H^1]NMR showed insignificant conversion. A similar reaction was performed by altering R_2 to a methyl group in **imine-2** and after two hours, [H^1]NMR showed a molar ratio of the corresponding aminosilane to amine of 2:1, an improvement over the $Ni(COD)_2$ system. Although the results of the bulkier imine showed no improvement, possibly due to sterics, the smaller imine showed improved selectivity for the desired aminosilane. Altering R_2 to an ethyl group in 4-methyl-N-(1-methylpropylidene)-benzenamine (**imine-3**) proceeds in four hours and showed exclusively aminosilane. Due to these interesting results, it was of interest to focus our efforts in understanding the $NiCOD(DMP)_2$ hydrosilylation system.

Mechanism

In order to probe the mechanistic behavior of our catalytic system, it was necessary to react the Ni-catalyst **2** with stoichiometric amounts of reactants. To reiterate, in regards to time increments captured with [H^1]NMR, it was observed that the aminosilane is formed first, followed by evolution of amine. A study was performed in which **2** dissolved in deuterated benzene was subjected to an excess of H_2. It was proposed that oxidative addition of H_2 may occur[23] followed by insertion of the isocyanide ligand [24] as shown (Scheme 4). [H^1]NMR after H_2 exposure, however, indicated no reaction had taken place and **2** remained unperturbed.

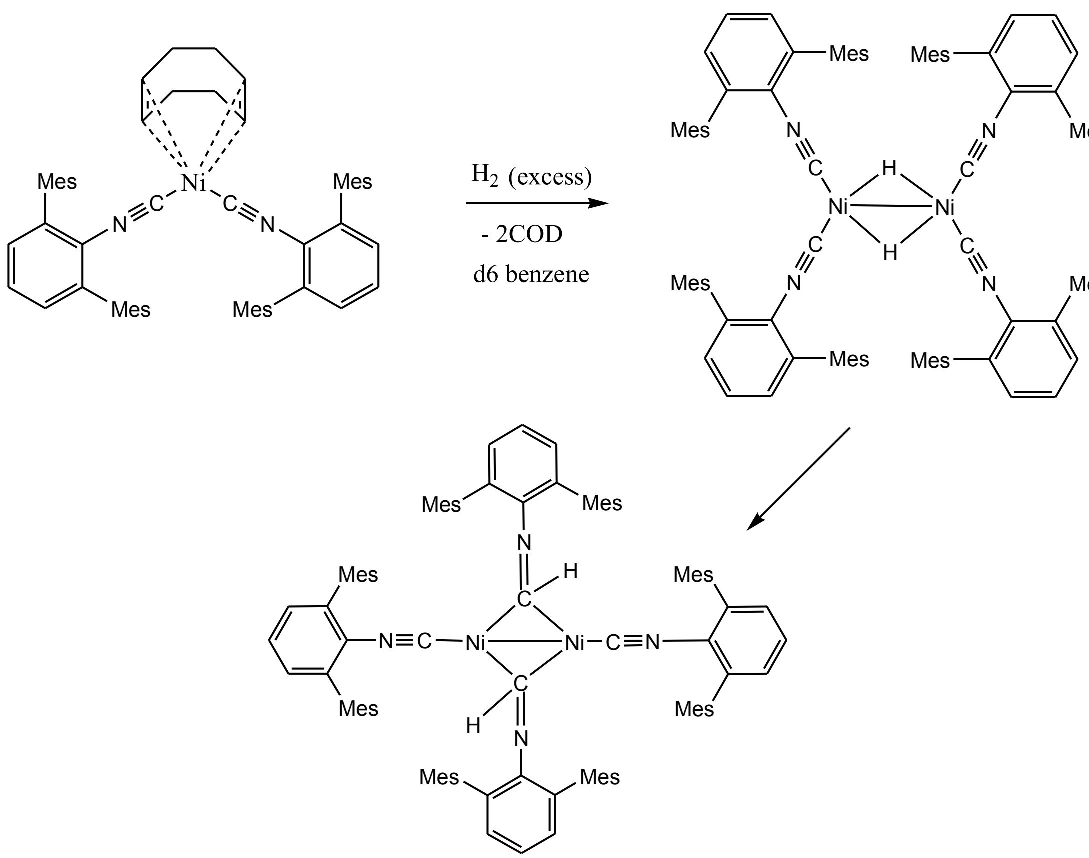

Scheme 4. Proposed dihydrogen insertion into NiCOD(DMP)2.

Another control experiment was carried out using **2** and a stoichiometric amount of the **imine-2**. No reaction was observed after weeks by [H^1]NMR. A separate mixture of catalyst and a stoichiometric amount of imine in deuterated benzene was subjected to excess H_2. It was proposed that amine should be formed, however, all components remained unreacted. Based upon this observation, it was clear that the silane is the key component in the catalytic system and that any H_2 generated *in situ* did not contribute to hydrogenation of the imine to amine in the presence of catalyst.

Although no interaction was witnessed between the nickel catalyst and imine by [H^1]NMR, it has been shown that it could weakly coordinate η-2 to the C-N, more so if R_1 is more electron-withdrawing[25]. The first step of the proposed catalytic cycle may involve a weak coordination of the imine to the Ni-catalyst. When the silane is introduced, oxidative addition of the silane by Ni(0) most likely takes place. Complexes have been previously characterized of this nature[26-30]. It was of interest to try and isolate the oxidative addition intermediate by reacting a stoichiometric amount of primary silane with the Ni-catalyst. However, many attempts at isolating such an intermediate proved fruitless, yet led into understanding an important proponent of the catalytic system being dehydrocoupling.

Once oxidative addition occurs of the silane, the next step most likely follows a Chalk-Harrod hydrosilylation mechanism[31] where the weakly coordinated imine will insert into the Ni-H bond via hydrometalation. This insertion is proposed to occur rather than silylmetalation, (Scheme 5), in which the imine inserts into the Ni-Si bond. After insertion, reductive elimination gives the desired aminosilane completing the cycle and regenerating the active Ni(0) catalyst (Scheme 6).

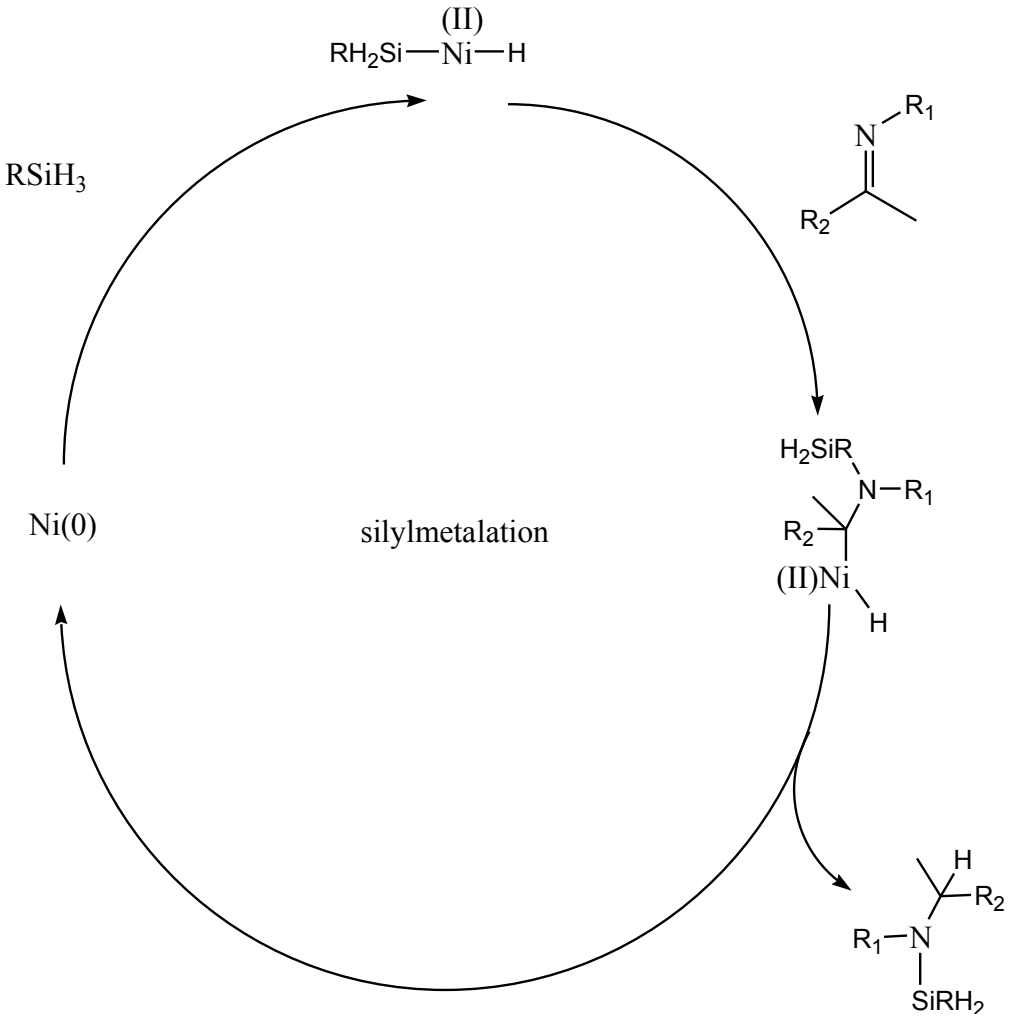

Scheme 5. Silylmetalation mechanism.

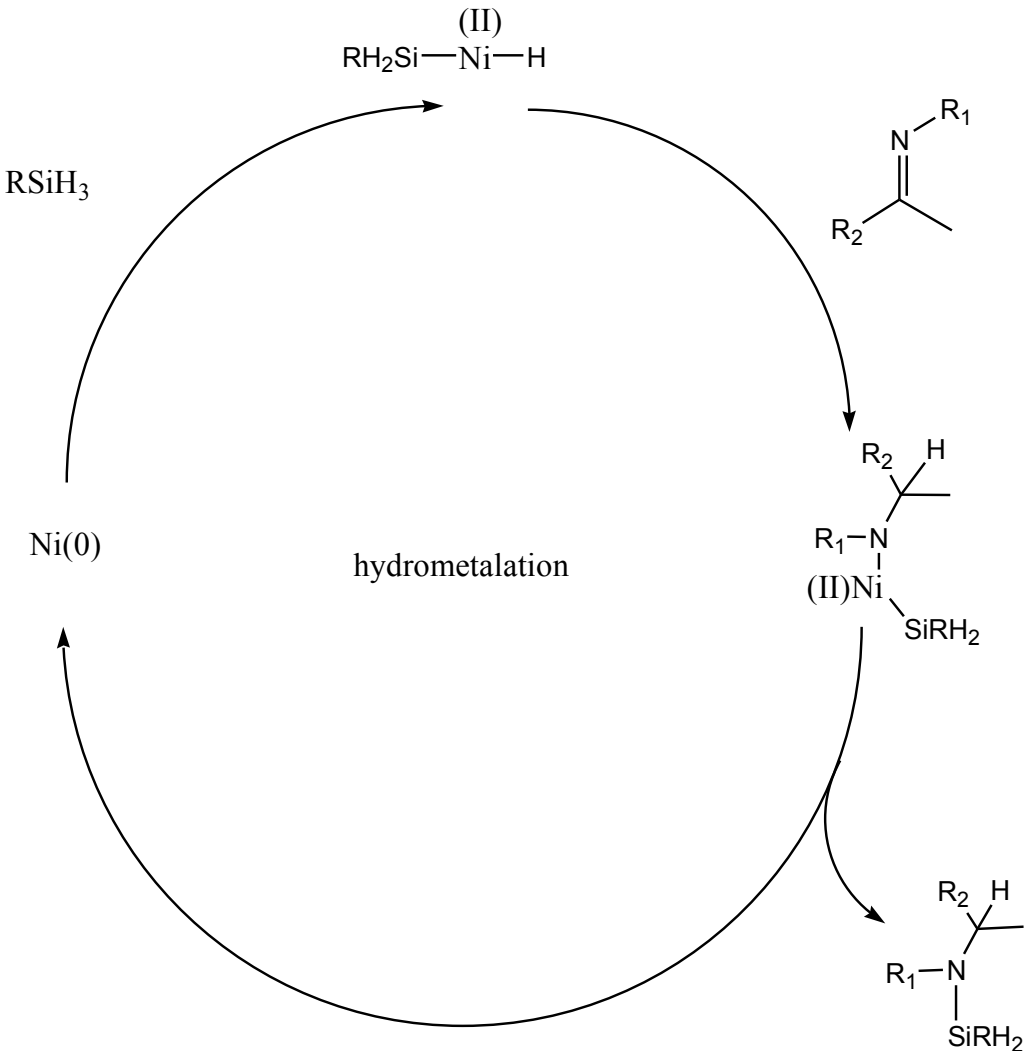

Scheme 6. Hydrometalation mechanism.

Dehydrocoupling

Of interest is the formation of polysilanes through the use of primary or secondary silanes using catalysts[32]. Catalysis through transition metals, specifically nickel, is efficient and Smith *et al.* report a bis(phospino)ethane nickel dimer with bridging hydrides that efficiently dehyrocouples via a proposed σ-bond metathesis mechanism [33]. In another report, Tanabe *et al.* report a bis(phospino)ethane nickel complex that efficiently dehydrocouples primary silanes to form polysilanes[34], and Schmidt *et al.* report a nickel NHC complex that does the same[35]. It was advantageous for us to carry out some dehydrocoupling studies of our own.

The first reaction done was the addition of phenylsilane to a stoichiometric moiety of **1** in deuterated benzene (Scheme 7) in which hydrogen evolution and change in color of the reaction mixture from yellow to a dark red-brown were observed. Analysis by [H^1]NMR was in agreement with literature for the formation of cyclic and linear polysilane chains in the range of 4.96-5.86ppm and 4.28-4.90ppm respectively[35]. It was found that some phenylsilane remained unreacted due to the catalyst being exhausted. **1** does exhibit instability at room temperature which shows why others may have used ligands such as phosphines or NHCs to increase the catalyst life-span. In this respect, we wanted to explore the extent of which **2** could perform dehydrocoupling. To a stoichiometric moiety of **2** in deuterated benzene was added phenylsilane and the reaction was analyzed by [H^1]NMR. Interestingly, the extent of dehydrocoupling that was observed for the $Ni(COD)_2$ system was not observed for the $NiCOD(DMP)_2$ system. Instead, diphenylsilane, as the redistribution product (Si-H observed at 5.08ppm), and diphenyldisilane (Si-H observed at 4.48ppm), as the dehydrocoupling product, were identified as the major products. The catalyst was exhausted after one hour.

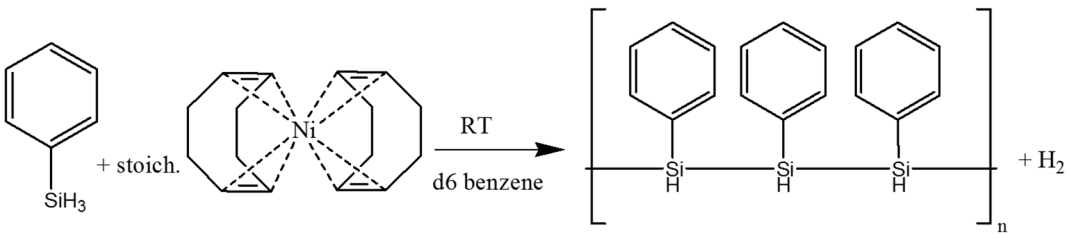

Scheme 7. Dehydrocoupling reaction.

It was of interest to then explore the dehydrocoupling of another primary silane. To a stoichiometric moiety of **1** in deuterated benzene was added hexylsilane. After four hours, the dehydrocoupling product dihexyldisilane (Si-H observed at 3.88ppm) was observed as the major product by [H^1]NMR. In similar fashion, to a stoichiometric moiety of **2** in deuterated benzene was added hexylsilane. [H^1]NMR showed the disappearance of catalyst after four hours along with unidentifiable products appearing to be of non-dehydrocoupling in character. In another experiment, to a stoichiometric moiety of **2** in anhydrous diethyl ether was added hexylsilane and the reaction was immediately chilled to -30°C. Over the course of a day, crystals were harvested yet determined by [H^1]NMR to be starting material. When the reaction mixture was warmed to room temperature, its characteristic vibrant orange turned to a dark red-brown. Analysis by GC-MS showed no evidence of starting material and products were unidentifiable, however, this study showed that the reaction did not proceed at colder temperatures.

Here we realized that the use of either phenylsilane or hexylsilane did make a significant difference in the outcome of the dehydrocoupling experiments for the two catalysts owing in part to possibly sterics or electronics, or a combination of both. It would be of value to do future testing of cyclohexylsilane in the same manner for a comparison of its degree of dehydrocoupling. Nonetheless, it was advantageous for us to mitigate the degree of

dehydrocoupling in hopes that the presiding degree of hydrosilylation would favor the formation of the desired aminosilane.

In another study, to a stoichiometric moiety of **2** in deuterated benzene was added diphenylsilane. It was proposed that diphenylsilane in the presence of **2** could undergo homo-coupling to form diphenylpolysilanes with the liberation of dihydrogen, or oxidative addition and form either one of two complexes being Ni(II) and Ni(I) (Scheme 8). The Ni(II) and Ni(I) complexes are analogous to those reported by Schimdt *et al*[35].

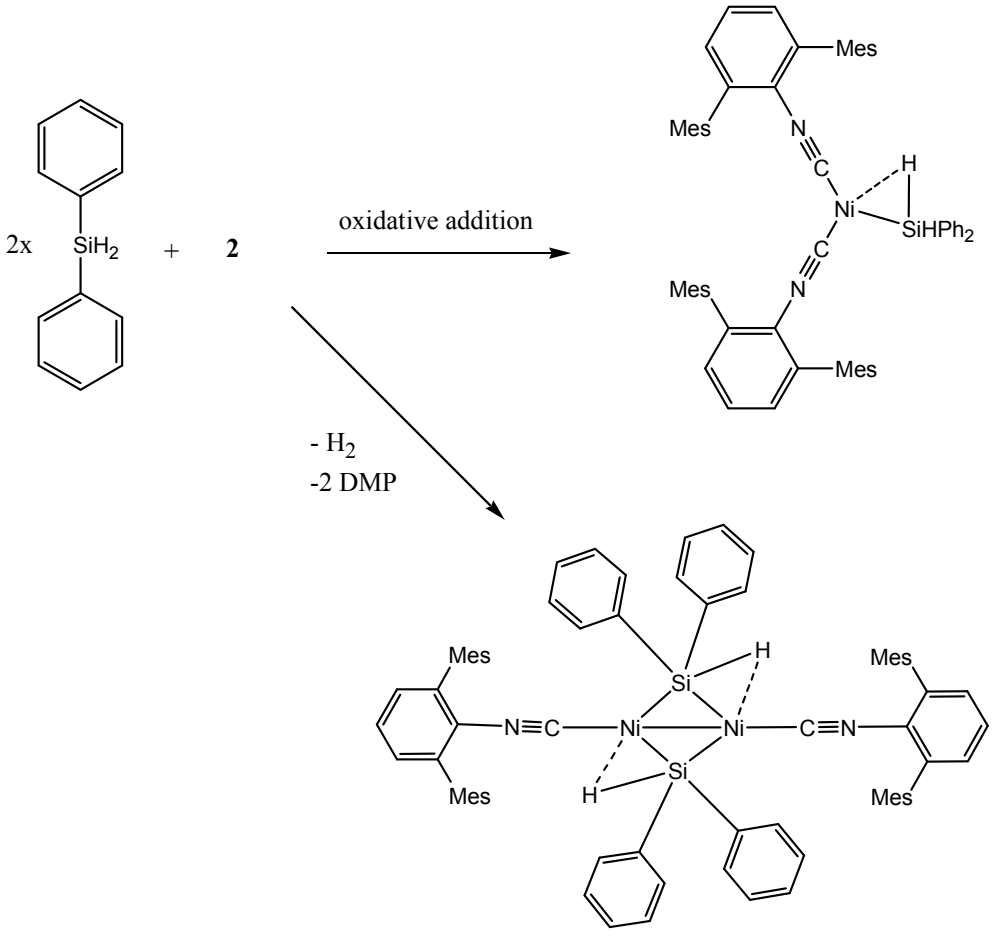

Scheme 8. Proposed diphenylsilane reaction with NiCOD(DMP)2.

Indeed, analysis by [H^1]NMR after a few days showed peaks shifted up field from -0.397 to -4.085ppm. In another experiment, to a stoichiometric moiety of **2** in anhydrous diethyl ether was added diphenylsilane and the reaction was immediately chilled to -30°C. Over the course of a day, crystals were harvested yet determined to be starting material showing that the reaction proceeds slow at chilled temperatures. Darker crystals were harvested after a few weeks and determined to be the result of 1,1-disilylation of one of the isocyanide ligands. The opposing isocyanide ligand bonds normally, yet, one of the mesityl rings bonds η-2 to the nickel to result in a 16e^-, Ni(0) complex (Figure 2). The bond length of C00W-N007 = 1.390(3) and vibrational stretch lies at 1428 cm^{-1} putting it somewhere between a double bond and a single bond (note: a squeeze was used in refinement to eliminate disorder of diethyl ether in the structure). [H^1]NMR of a mixture of dark crystals and **2** shows an up field shift at -0.387ppm that could not be assigned. The Si-H peak is evident at 5.09ppm. Future studies will be carried out to determine if this 1,1-disilylation complex demonstrates any catalytic behavior.

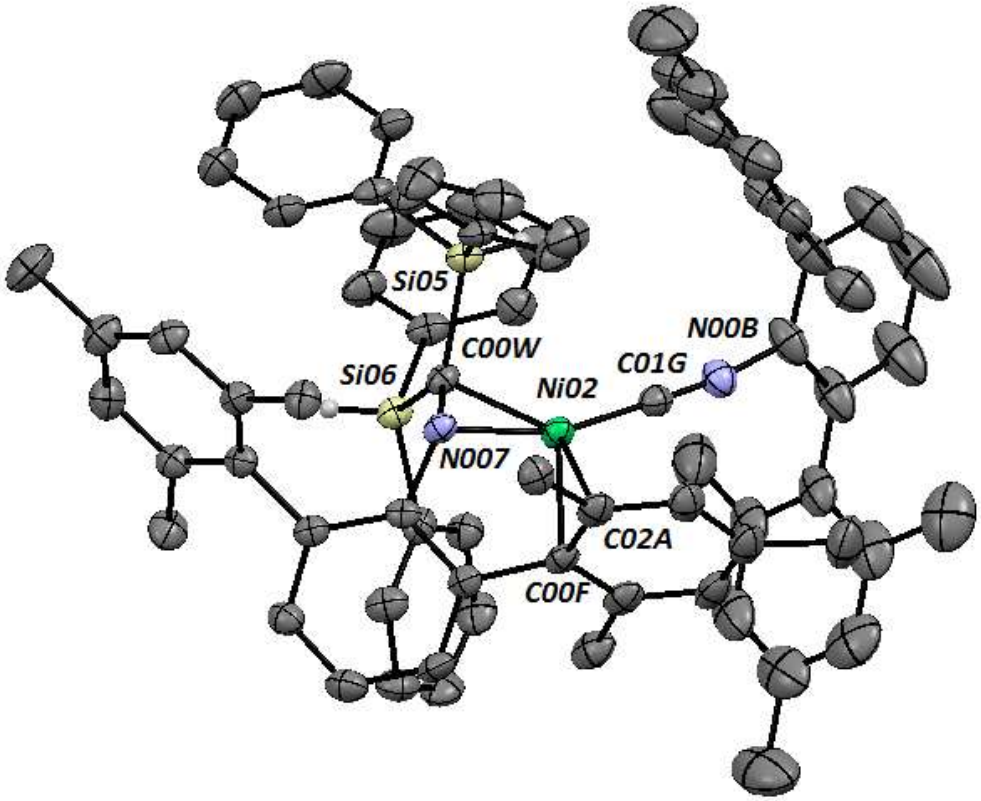

Figure 2. Crystal structure of 1,1-disilylation product $Ni(Ph_2SiH)_2(DMP)_2$.

The proposed mechanism for 1,1-disilylation complex is shown (Scheme 9).

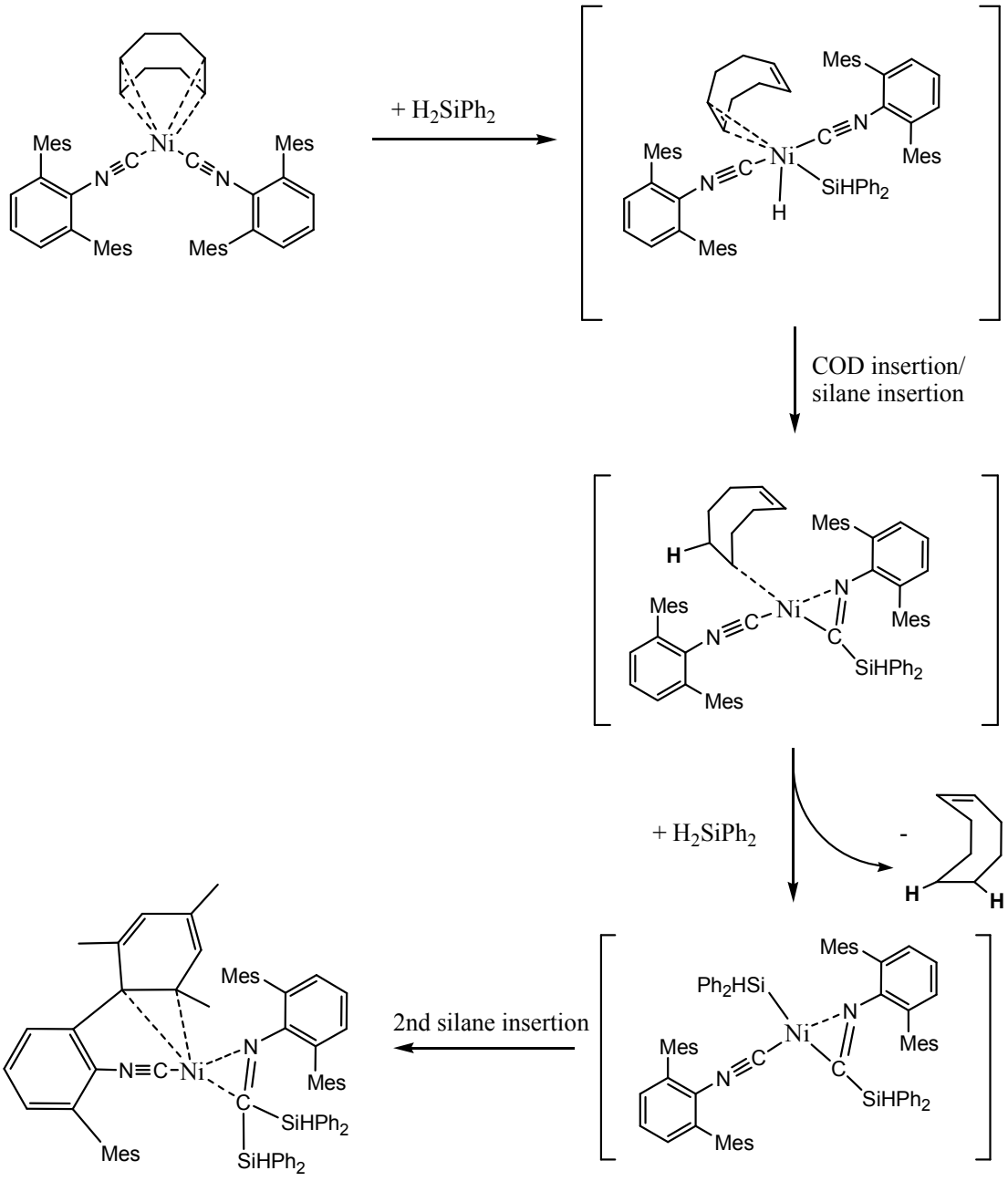

Scheme 9. 1,1-disilylation proposed mechanism.

Hexysilane

With a grasp on how to mitigate the extent of dehydrocoupling of the Ni(0) catalyst system using hexylsilane as opposed to phenylsilane, we now wanted to explore our hydrosilylation system of interest. To a solution of 2.5% molar loading of **2**, dissolved in deuterated benzene was added **imine-2**, followed by drop-wise addition of a solution of hexylsilane (Gelest brand) in deuterated benzene. The reaction was monitored by [H^1]NMR after 30 minutes and showed complete conversion of **imine-2** and remarkably complete selectivity for the desired aminosilane.

Having gained selectivity for the desired aminosilane, it was necessary to expand the scope of the NiCOD(DMP)$_2$/hexysilane system. Imines of 4-**X**-N-(1-methylethylidene)-benzenamine structure were explored by altering the para-X group (Scheme 10) with different functional groups and reaction times are specified (Table 1).

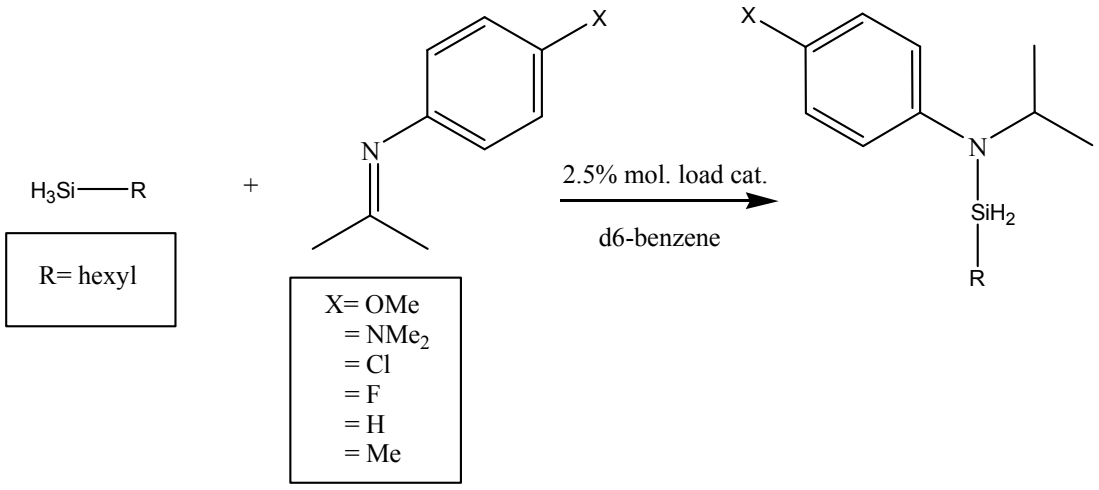

Scheme 10. Scope reaction scheme.

Para-X group	conversion≠	Time (hr)
H*	complete	2
Me*	complete	0.5
OMe*	complete	3
Cl	complete	2
F#	complete	2
NMe_2	complete	2

Figure 3. Conversion times for varying para-X groups.

≠conversion determined by [H^1]NMR

*imines isolated in 50% purity (impurity is corresponding para-functionalized aniline)

#imine isolated in 66% purity

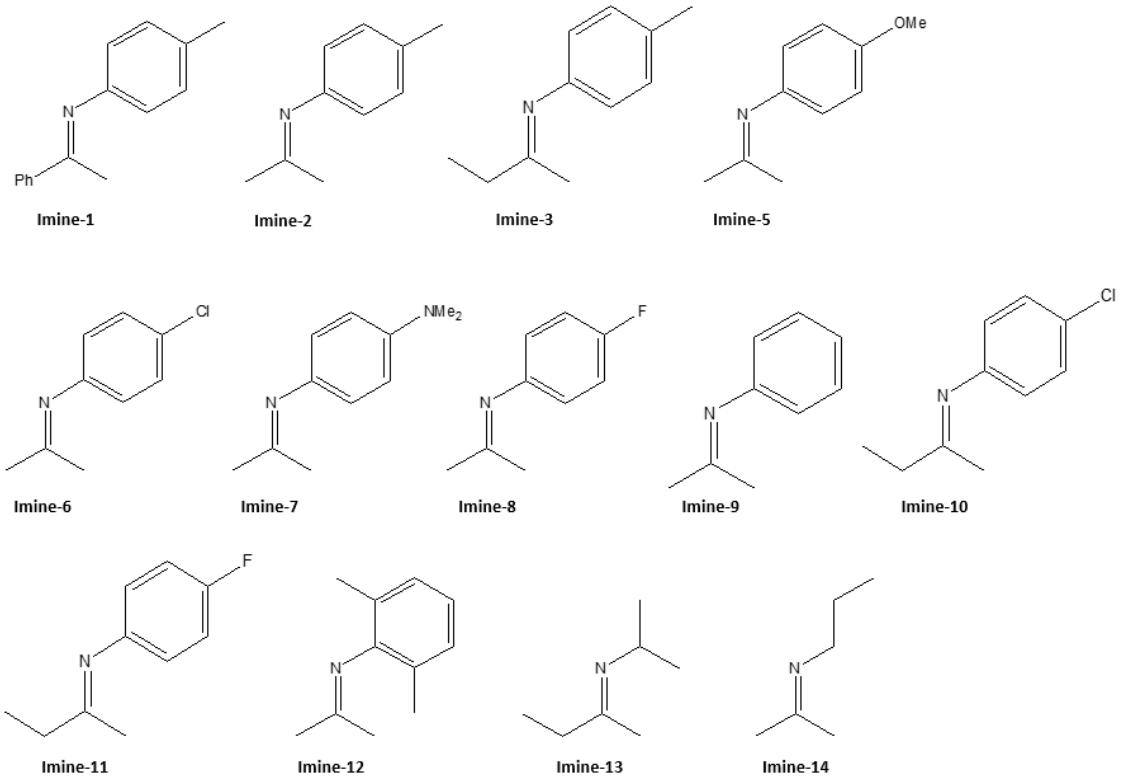

Figure 4. Structures of imines.

As concluded from the scope study, there was no difference in reaction rates for electron-donating versus electron-withdrawing groups (i.e. X=NMe_2 versus X=F). Both were complete in two hours and selective for the aminosilane. The para-methyl system was the fastest with conversion complete after 30 minutes as oppose to three hours for the para-methoxy. As a control in determining if the selectivity of the aminosilane is gained primarily by the use of hexylsilane, a reaction was set up using **1** as the catalyst in the presence of **imine-2**. Selectivity for the aminosilane was lost, and the reaction did not proceed to completion when compared to **2** after two hours. **Imine 3,** 4-methyl-N-(1-methylpropylidene)-benzenamine, showed a slower conversion time (although complete conversion) than its 4-methyl-N-(1-

methylethylidene)- benzenamine, **imine-2**, counterpart due in most part to sterics. 4-chloro-N-(1-methylpropylidene)-benzenamine, **imine-10** and 4-fluoro-N-(1-methylpropylidene)-benzenamine, **imine-11** both proceed similar to **imine-3**. The sterically encumbered 2,4-methyl substituted imine (**imine-12**) indeed showed diminished reactivity.

In separate experiments, when R_1 of the imine is an alkyl group (e.g. isopropyl, tert-butyl or sec-butyl) the conversions were very slow. When R_1 was changed to n-propyl, remarkably full conversion to the aminosilane was obtained in two hours. In another interesting respect, imines that contained their analogous unreacted aniline starting material seemed to be unperturbed, as hydrosilylation readily proceeds, a testament to the selective character of catalyst **2** participating in hydrosilylation, and not in dehydrocoupling.

The scope of imines was repeated to gain insight as to the extent of conversion of hydrosilylation by using a premeasured reference to compare with aminosilane generated. As done previously, the conversion was presumed to be complete by the complete disappearance of imine. To a catalytic amount of **2** was added 1mL of a stock solution of 0.062M hexylmethylbenzene in deuterated benzene. Next, the desired imine was added directly followed by drop-wise addition of a solution of hexylsilane in 1mL of deuterated benzene. Upon addition of silane, the formation of bubbles was observed and the reaction was agitated with a magnetic stir bar for the extent of 2 hours. After the allotted time, an aliquot (0.10mL) was taken and diluted with approximately 0.40mL of deuterated benzene. [H^1]NMR was taken and the extent of hydrosilylation was determined with regard to the hexylmethylbenzene reference. Surprisingly, conversions were not as high as first anticipated showing between 70-30%.

Some factors that may contribute to inaccurate conversion percentages may be inaccurate purity of the imines. Imine purity was determined by [H^1]NMR, however, GC may be a better means of determining purity of the imines. It is evident that in the repeated scope experiments, the imine was observed to be completely exhausted after 2 hours by [H^1]NMR.

The limitation of accurately determining conversion by GC-MS was the observation that the Si-N bond was cleaved when subject to the GC column and only the amine was observed. Terminal –OH groups in the column could participate in alcoholysis of the aminosilane, generating the more stable Si-O species with liberation of the free amine. In another regard, upon removing volatiles from the reaction mixture in the presence of catalyst, the aminosilane was also cleaved to form the amine. The catalyst may still be active at this point and methods are being undertaken to selectively deactivate the catalyst without affecting the aminosilane generated in the reaction mixture. A process for isolation of pure aminosilane is still in development.

Active Ni Catalyst

It was essential at this point to explore why the Ni(0)L_2 system has an advantage over the Ni(0) system and in doing so, it was necessary to understand the possible interaction the imine/silane might have with the m-terphenyl isocyanides of the catalyst. HCl (1M in diethyl ether) was used as a surrogate for silane and added in a stoichiometric amount to **2** dissolved in diethyl ether at room temperature and showed immediate evolution of a precipitate. Although efforts to recrystalize the precipitate from THF were unsuccessful, filtration of the reaction mixture and recrystalization at -30°C produced single crystals that were solved by x-ray diffraction as the following (Figure 4):

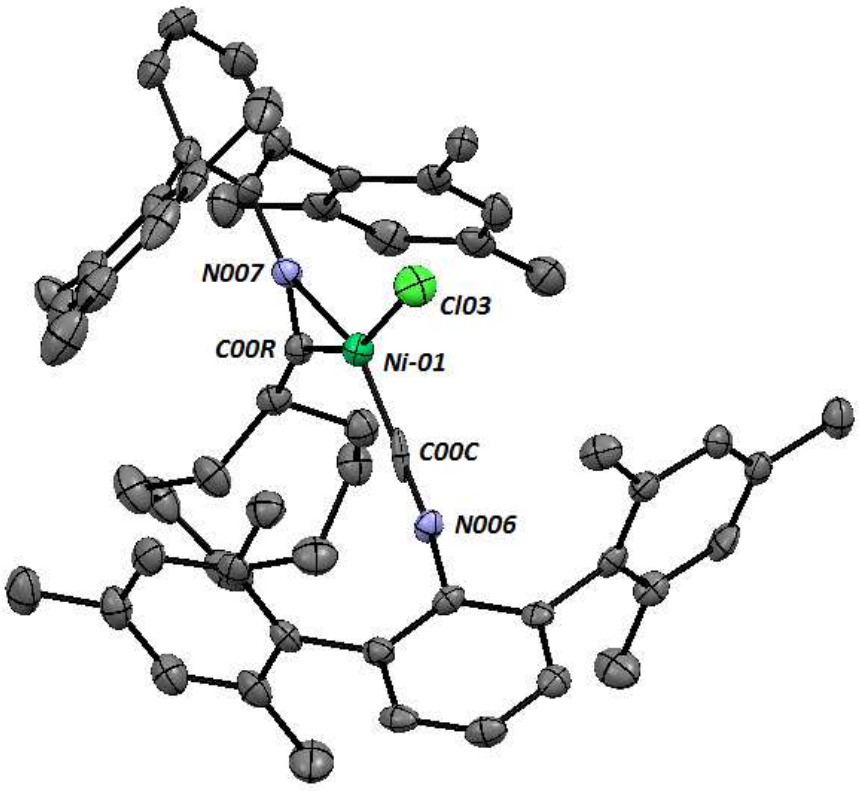

Figure 5. Crystal structure Ni(II) insertion complex NiCOECl(DMP)$_2$.

The following structure revealed some known behavior of isocyanide insertion into the Ni-H bond[36]. Similar insertion of the isocyanide may lead to an active catalyst after oxidative addition of the silane to form the respective Ni(II). In order to give validity to such a claim, our next objective was to obtain the Ni-Si-iminoacyl or the Ni-H-iminoacyl, whether the proton or silane is reductively substituted to COD to form the cyclooctene or silaoctene respectively. A reaction was run of hexylsilane and a stoichiometric amount of **2** in deuterated benzene and run GC-MS. There was, however, no evidence that the hexylsilaoctene had formed.

It is proposed that oxidative addition of the silane will form the Ni(II) species first, followed by insertion of the cyclooctadienyl ligand into the Ni-H bond to form the corresponding Ni(II) silane. This is followed by insertion of the isocyanide into the Ni-C bond of the inserted cyclooctadienyl ligand. The resulting iminoacyl complex could undergo reductive elimination to yield the disubstituted imine and Ni(0)L. This short lived complex could be the active catalyst (Scheme 11).

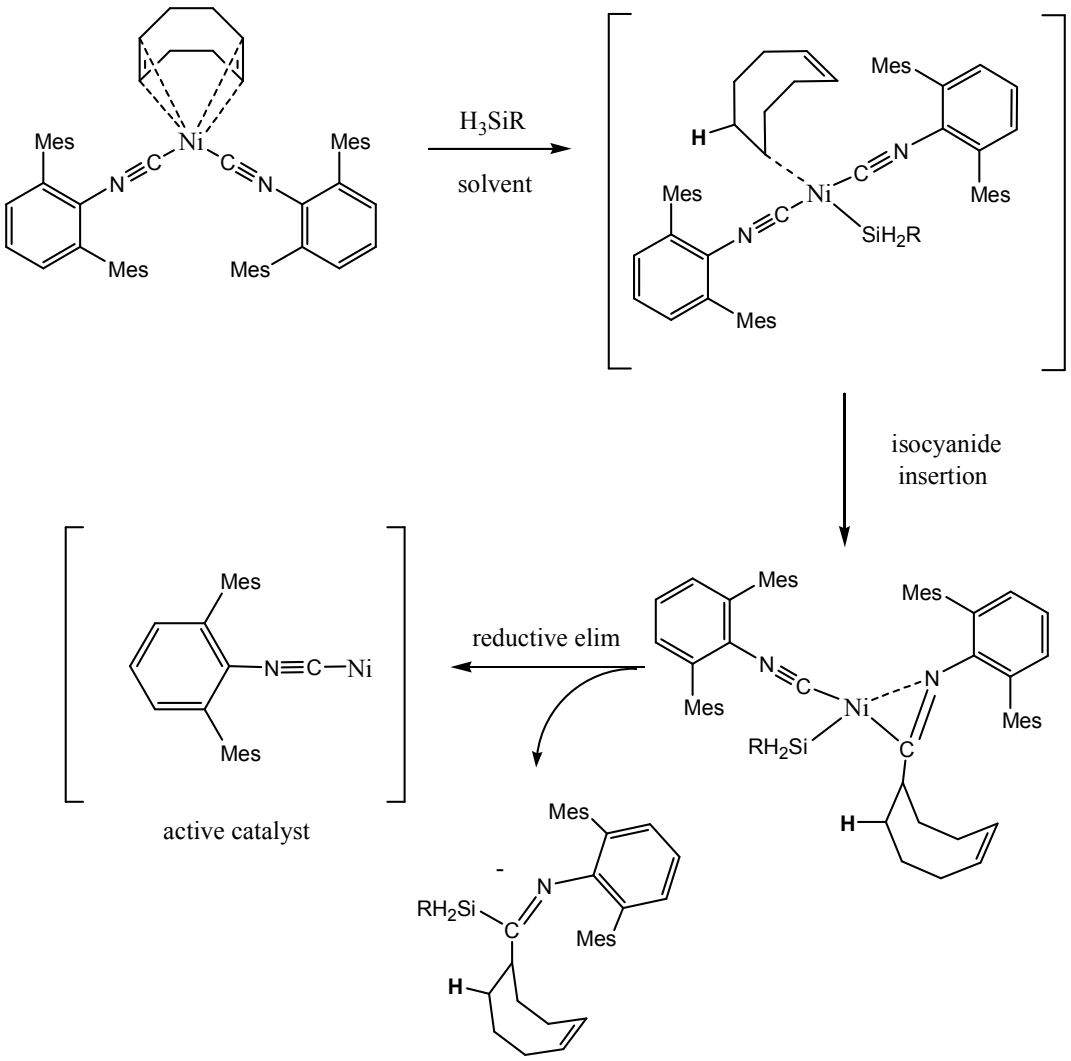

Scheme 11. Proposed mechanism leading to active catalyst.

The active catalyst could then interact with imine and undergo oxidative addition with silane. The imine would then insert into the Ni-H bond generating a Ni-amine. Reductive elimination would generate the desired aminosilane and regenerate the active Ni(0)L catalyst (Scheme 12).

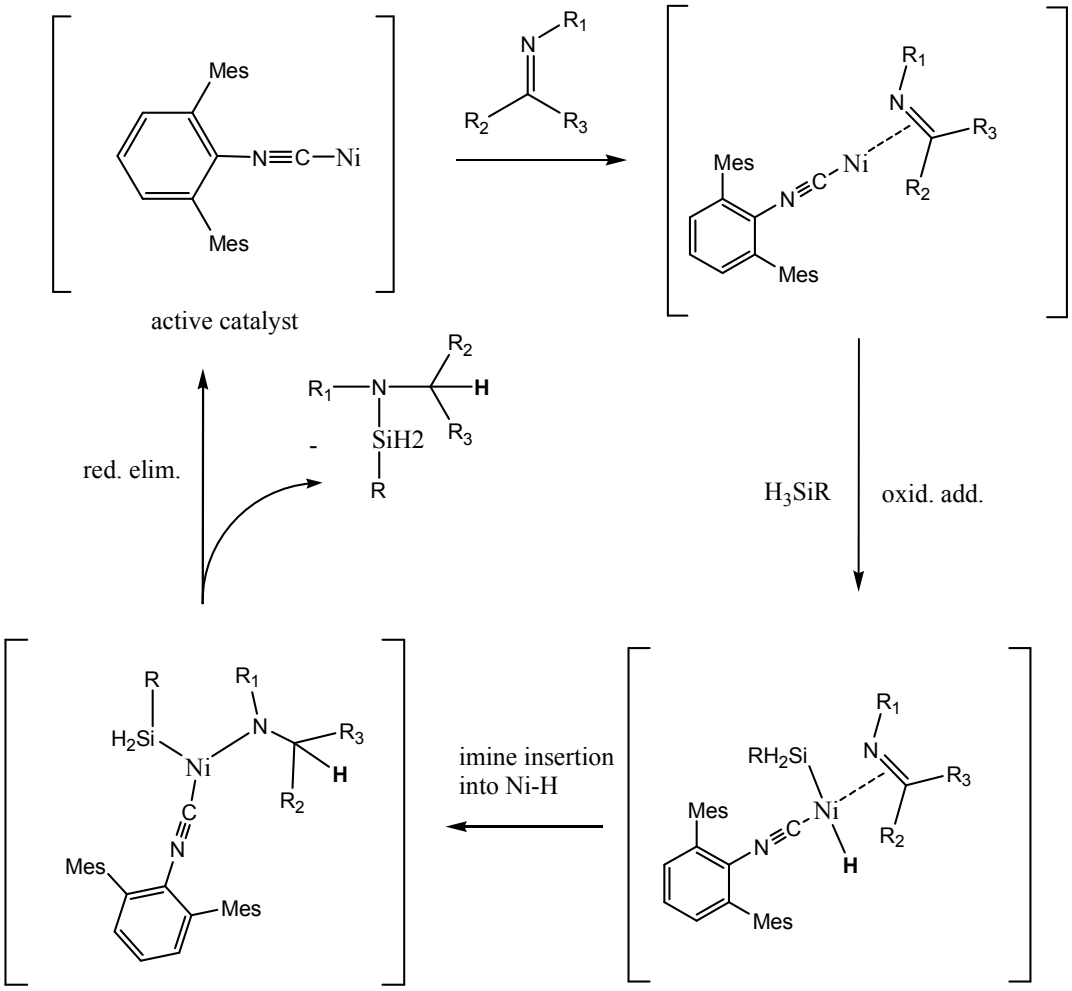

Scheme 12. Proposed mechanism revised for insertion.

Attempts were made to observe a Ni-silyl complex by reacting **2** with a stoichiometric amount of the tertiary silane, triethylsilane. However, the triethylsilane/NiCOD(DMP)$_2$ reaction was stagnant at -30°C for many weeks. In similar fashion, a structure was sought regarding the reaction of hexylsilane with a stoichiometric amount of **2** at -30°C, however, only crystals of starting material were obtained. After a few weeks, the mother liquor darkened, however, no crystals were harvested.

Ni(II) species

Interestingly, in an attempt to oxidatively add a chlorosilane in similar manner to Smith *et al*[33], the addition of $HSiCl_3$ to a stoichiometric amount of **2** generated colorless crystals determined by x-ray diffraction to be the following species (Figure 5). The Ni-H species was not characterized, however, cyclooctene as the reduced species, was characterized by GC-MS (Scheme 13):

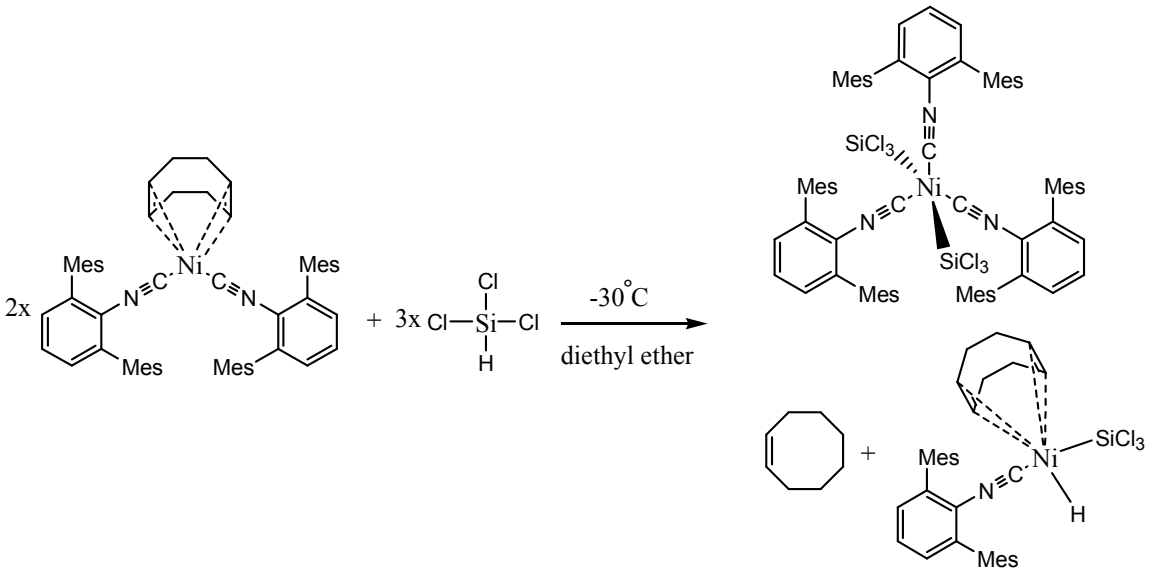

Scheme 13. Reaction scheme of $Ni(SiCl_3)_2(DMP)_3$

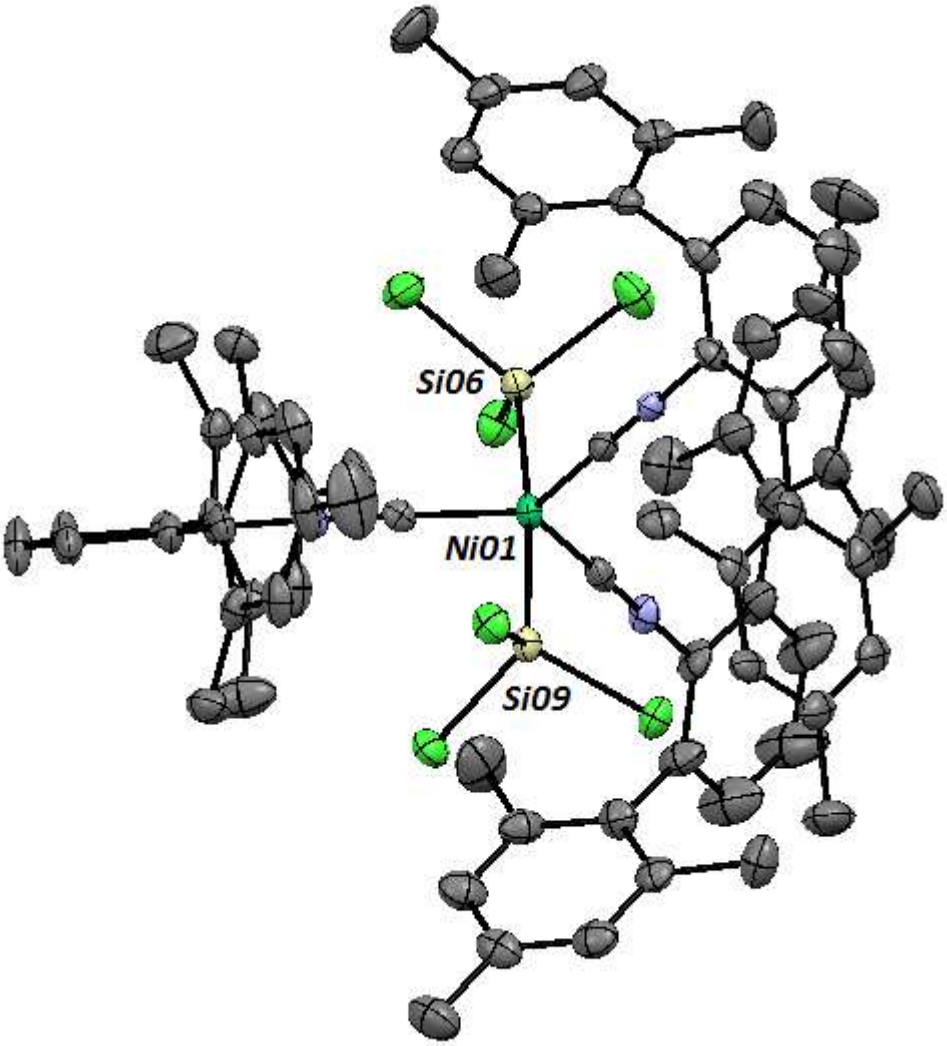

Figure 6. Crystal structure of $Ni(SiCl_3)_2(DMP)_3$ (note: one equivalent of diethyl ether was left out for clarity).

Similarly, $HGeCl_3$ can be added in much the same manner to generate the analogous species. Again, the Ni-H species was not characterized, however, cyclooctadiene was characterized by GC-MS giving credence that H_2 is liberated (Scheme 14):

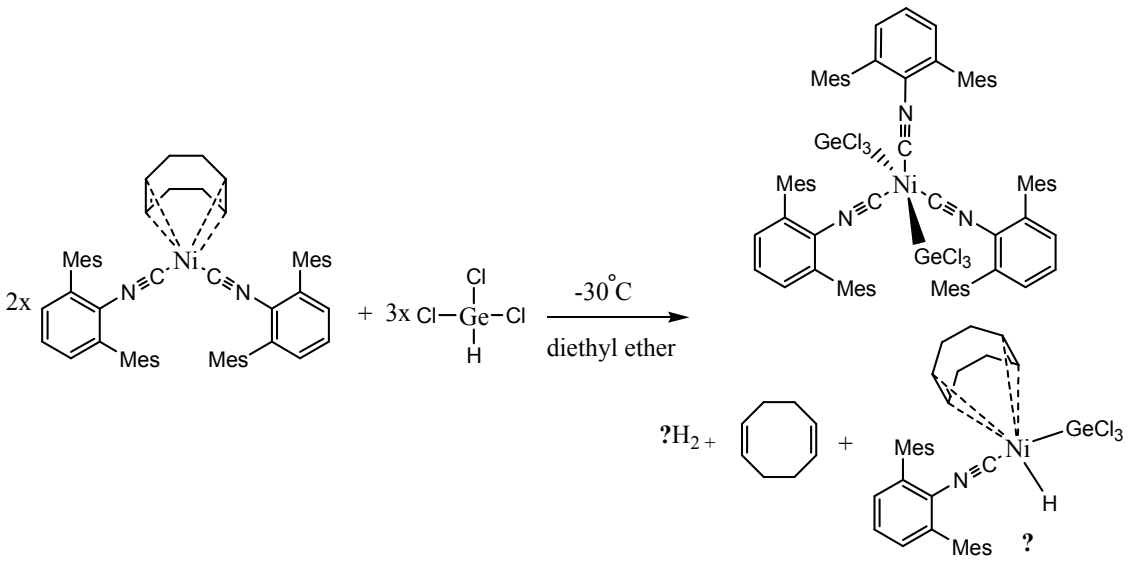

Scheme 14. Reaction scheme of $Ni(GeCl_3)_2(DMP)_3$.

Analogous bonding motif structures are reported[37]

Supporting Data

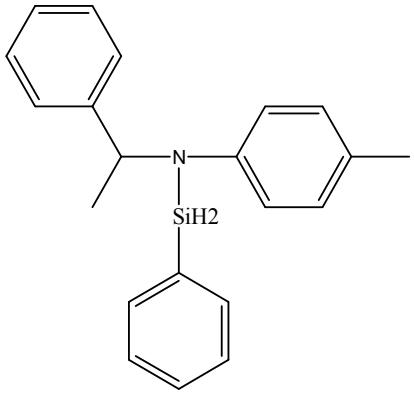

Aminosilane 1

^{1}H NMR (400 MHz, C_6D_6, 298K): δ 7.59-7.57 (m, 2H), 7.27 (d, 2H, *J* = 7.6Hz), 7.18-7.02 (m, 6H), 6.96 (d, 2H, *J* = 8.4Hz), 6.83 (d, 2H, *J* = 8.8Hz), 5.35 (s, 2H), 4.76 (q, 1H, *J* = 7.2Hz), 2.04 (s, 3H), 1.55 (d, 3H, *J* = 7.2Hz).

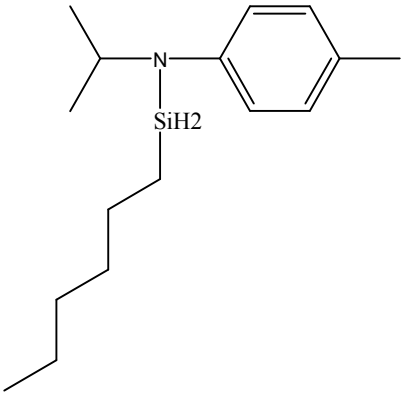

Aminosilane 2

^{1}H NMR (400 MHz, C_6D_6, 298K): δ 6.99 (s, 4H), 4.86 (t, 2H, *J* = 3.2Hz), 3.59 (sept, 1H, *J* = 6.8Hz), 2.15 (s, 3H), 1.17 (d, 6H, *J* = 6.4Hz), 1.29-1.20 (m, 8H), 0.86 (t, 3H, *J* = 7.2Hz), 0.78 (m, 2H).

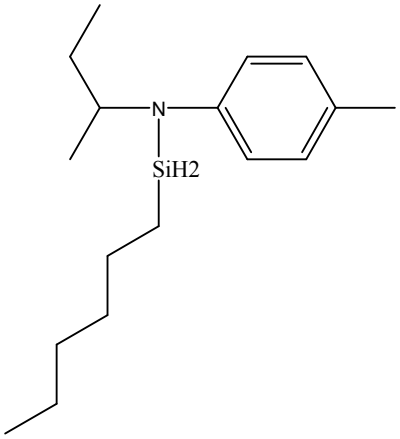

Aminosilane 3

^{1}H NMR (400 MHz, C_6D_6, 298K): δ 6.99 (s, 4H), 4.86 (m, 2H, *J* = 9.6Hz), 3.28 (sextet, 1H, *J* = 6.8Hz), 2.14 (s, 3H), 1.70-1.61 (m, 2H), 1.33-1.18 (m, 8H), 1.19 (d, 3H, *J* = 6.8Hz), 0.89 (t, 3H, *J* = 7.2Hz), 0.86 (t, 3H, *J* = 6.8Hz), 0.79 (m, 2H).

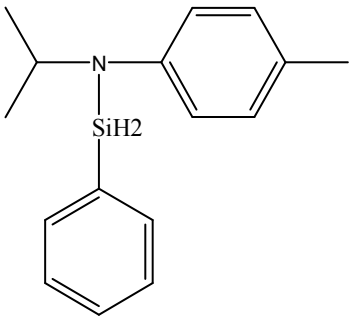

Aminosilane 4

^{1}H NMR (400 MHz, C_6D_6, 298K): δ 7.50 (d, 2H, *J* = 7.6Hz), 7.16-7.11 (m, 3H), 6.86 (d, 2H, *J* = 8.0Hz), 6.56 (d, 2H, *J* = 8.0Hz), 5.34 (s, 2H), 3.67 (sept, 1H, *J* = 6.8Hz), 2.09 (s, 3H), 1.16 (d, 6H, *J* = 6.8Hz).

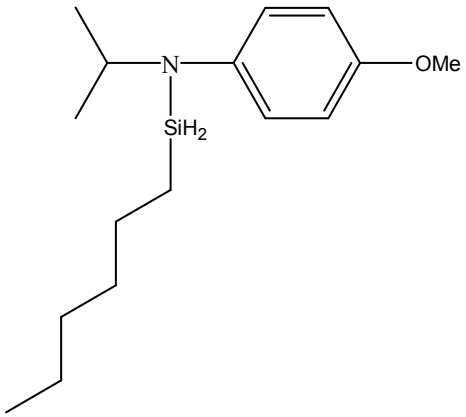

Aminosilane 5

^{1}H NMR (400 MHz, C_6D_6, 298K): δ 6.99(d, 2H, *J* = 8.8Hz), 6.76 (d, 2H, *J* = 8.8Hz), 4.87 (t, 2H, *J* = 3.2Hz), 3.52 (sept, 1H, *J* = 6.8Hz), 3.33 (s, 3H), 1.15 (d, 6H, *J* = 6.8Hz), 1.30-1.18 (m, 8H), 0.76 (m, 2H).

(note: could not locate the (t, 3H) of the terminal methyl of the hexyl substituent due to overlap with residual hexylsilane)

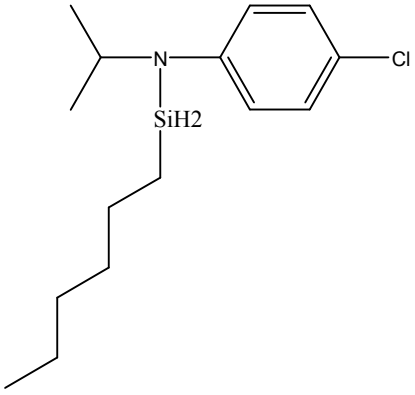

Aminosilane 6

^{1}H NMR (400 MHz, C_6D_6, 298K): δ 7.10 (d, 2H, *J* = 8.8Hz), 6.70 (d, 2H, *J* = 8.8Hz), 4.70 (t, 2H, *J* = 3.2Hz), 3.40 (sept, 1H, *J* = 6.8Hz), 1.38-1.10 (m, 8H), 1.06 (d, 6H, *J* = 6.4Hz), 0.87 (t, 3H, *J* = 6.8Hz), 0.66 (m, 2H).

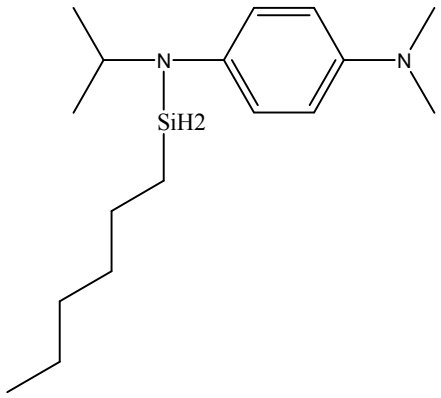

Aminosilane 7

^{1}H NMR (400 MHz, C_6D_6, 298K): δ 7.09 (d, 2H, *J* = 8.4Hz), 6.60 (d, 2H, *J* = 8.8Hz), 4.94 (t, 2H, *J* = 3.2Hz), 3.58 (sept, 1H, *J* = 6.8Hz), 1.38-1.13 (m, 8H), 1.20 (d, 6H, *J* = 6.4Hz), 0.87 (t, 3H, *J* = 6.8Hz), 0.79 (m, 2H).

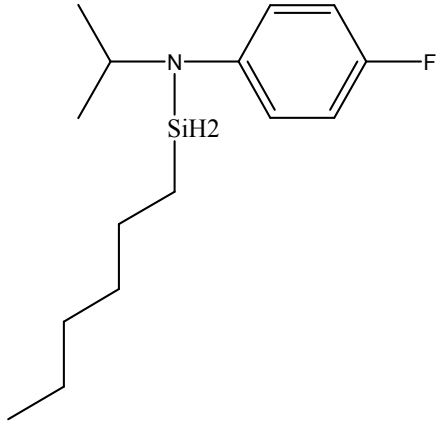

Aminosilane 8

^{1}H NMR (400 MHz, C_6D_6, 298K): δ 6.78 (d, 2H, *J* = 7.6Hz), 6.77 (d, 2H, *J* = 5.2Hz), 4.75 (t, 2H, *J* = 3.2Hz), 3.41 (sept, 1H, *J* = 6.8Hz), 1.35-1.14 (m, 8H), 1.07 (d, 6H, *J* = 6.8Hz), 0.87 (t, 3H, *J* = 6.8Hz), 0.69 (m, 2H).

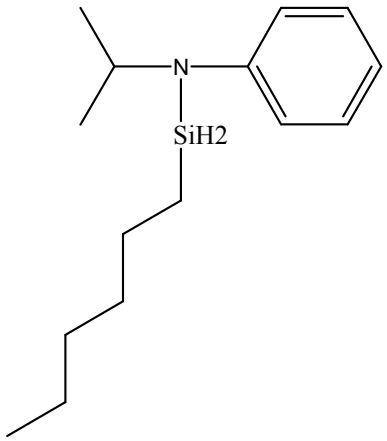

Aminosilane 9

^{1}H NMR (400 MHz, C_6D_6, 298K): δ 7.16 (t, 2H, *J* = 7.2Hz), 7.00 (d, 2H, *J* = 7.6Hz), 6.89 (t, 1H, *J* = 7.2Hz), 4.82 (t, 2H, *J* = 3.2Hz), 3.59 (sept, 1H, *J* = 6.8Hz), 1.35-1.14 (m, 8H), 1.16 (d, 6H, *J* = 6.8Hz), 0.87 (t, 3H, *J* = 6.8Hz), 0.77 (m, 2H).

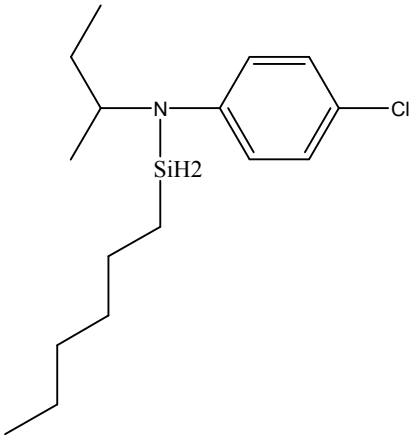

Aminosilane 10

^{1}H NMR (400 MHz, C_6D_6, 298K): δ 7.10 (d, 2H, *J* = 8.8Hz), 6.73 (d, 2H, *J* = 8.8Hz), 4.71 (m, 2H, *J* = 12.0Hz), 3.28 (sextet, 1H, *J* = 6.8Hz), 1.61-1.50 (m, 2H), 1.33-1.18 (m, 8H), 1.09 (d, 3H, *J* = 6.8Hz), 0.87 (t, 3H, *J* = 6.8Hz), 0.79 (t, 3H, *J* = 7.2Hz), 0.70 (m, 2H).

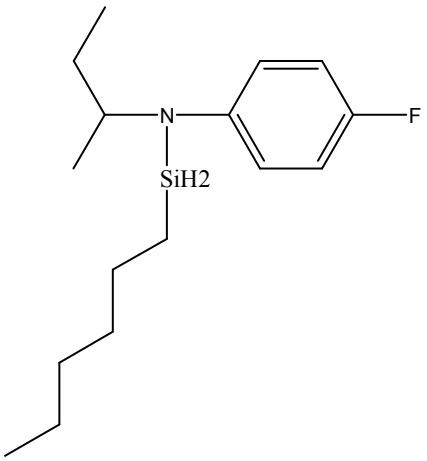

Aminosilane 11

^{1}H NMR (400 MHz, C_6D_6, 298K): δ 6.80 (d, 2H, *J* = 6.8Hz), 4.76 (m, 2H), 3.11 (sextet, 1H, *J* = 6.8Hz), 1.60-1.49 (m, 2H), 1.33-1.18 (m, 8H), 1.09 (d, 3H, *J* = 6.8Hz), 0.87 (t, 3H, *J* = 6.8Hz), 0.84 (t, 3H, *J* = 7.2Hz), 0.70 (m, 2H).

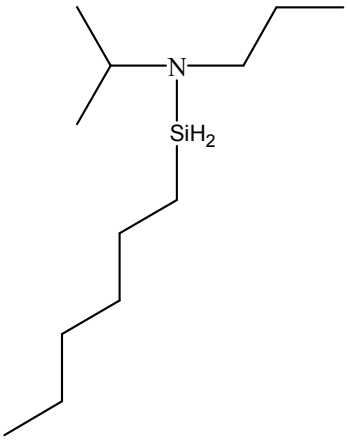

Aminosilane 12

^{1}H NMR (400 MHz, C_6D_6, 298K): δ 4.68 (t, 2H, *J* = 3.2Hz), 2.98 (sept, 1H, *J* = 6.8Hz), 2.69 (t, 2H), 1.33-1.19 (m, 8H), 1.08 (d, 6H, *J* = 6.8Hz), 0.99 (sextet, 2H), 0.90 (t, 3H), 0.82 (t, 3H, *J* = 7.2Hz), 0.74 (m, 2H).

Crystal data and structure refinement for $Ni(Ph_2SiH)_2(DMP)_2$.

Identification code	P21c_sq - Copy
Empirical formula	$C_{74}H_{72}N_2NiSi_2$
Formula weight	1104.22
Temperature/K	100.0
Crystal system	monoclinic
Space group	$P2_1/n$
a/Å	28.289(2)
b/Å	12.5062(10)
c/Å	40.006(3)
α/°	90
β/°	94.4080(10)
γ/°	90
Volume/$Å^3$	14111.7(19)
Z	8
$\rho_{calc}g/cm^3$	1.039
μ/mm^{-1}	0.347
F(000)	4688.0
Crystal size/mm^3	? × ? × ?
Radiation	MoKα (λ = 0.71073)
2Θ range for data collection/°	2.888 to 50.054
Index ranges	-33 ≤ h ≤ 30, -13 ≤ k ≤ 14, -46 ≤ l ≤ 47
Reflections collected	99750
Independent reflections	24914 [R_{int} = 0.0641, R_{sigma} = 0.0662]
Data/restraints/parameters	24914/0/1447
Goodness-of-fit on F^2	1.039
Final R indexes [I>=2σ (I)]	R_1 = 0.0523, wR_2 = 0.1265
Final R indexes [all data]	R_1 = 0.0900, wR_2 = 0.1437
Largest diff. peak/hole / e $Å^{-3}$	0.52/-0.40

Bond Lengths for P21c_sq - Copy.

Atom	Atom	Length/Å	Atom	Atom	Length/Å
Ni01	N008	1.879(2)	C01N	C029	1.379(4)
Ni01	C00H	1.998(3)	C01N	C02Z	1.514(4)
Ni01	C012	2.180(3)	C01O	C01V	1.393(4)
Ni01	C01A	1.803(3)	C01P	C022	1.404(4)
Ni02	N007	1.880(2)	C01P	C023	1.400(4)

Ni02	C00F	2.172(3)	C01Q	C02F	1.501(4)
Ni02	C00W	2.004(3)	C01Q	C03Q	1.384(4)
Ni02	C01G	1.801(3)	C01R	C02A	1.389(4)
Ni02	C02A	2.500(3)	C01R	C02N	1.391(4)
Si03	C00H	1.892(3)	C01S	C02U	1.389(4)
Si03	C00M	1.890(3)	C01T	C030	1.377(4)
Si03	C01I	1.875(3)	C01U	C032	1.380(5)
Si04	C00E	1.871(3)	C01V	C03J	1.501(4)
Si04	C00H	1.891(3)	C01W	C01Z	1.379(4)
Si04	C00Q	1.875(3)	C01W	C022	1.396(4)
Si05	C00P	1.878(3)	C01X	C024	1.385(4)
Si05	C00U	1.871(3)	C01Y	C02X	1.384(4)
Si05	C00W	1.895(3)	C01Z	C021	1.380(4)
Si06	C00W	1.888(3)	C020	C02G	1.385(4)
Si06	C01L	1.881(3)	C021	C023	1.385(4)
Si06	C01P	1.889(3)	C025	C038	1.383(4)
N007	C00G	1.412(3)	C026	C031	1.381(4)
N007	C00W	1.390(3)	C027	C02N	1.377(4)
N008	C00H	1.388(3)	C028	C02A	1.509(4)
N008	C00X	1.415(3)	C02B	C02W	1.389(4)
N009	C01A	1.175(3)	C02C	C032	1.374(4)
N009	C01B	1.403(3)	C02F	C02K	1.395(4)
N00B	C01G	1.172(3)	C02F	C02V	1.397(4)
N00B	C03H	1.395(4)	C02G	C03A	1.373(5)
C00C	C00G	1.411(4)	C02H	C02Q	1.372(4)
C00C	C00N	1.504(4)	C02I	C02L	1.377(4)
C00C	C00S	1.399(4)	C02J	C02P	1.389(4)
C00D	C00I	1.415(4)	C02K	C033	1.392(4)
C00D	C00O	1.394(4)	C02K	C04A	1.515(5)
C00D	C014	1.504(4)	C02L	C030	1.401(4)
C00E	C00L	1.391(4)	C02L	C03P	1.516(4)
C00E	C01F	1.398(4)	C02M	C02W	1.378(5)
C00F	C00T	1.429(4)	C02M	C031	1.384(5)
C00F	C00Y	1.507(4)	C02N	C03T	1.520(4)
C00F	C02A	1.423(4)	C02O	C03E	1.406(5)
C00G	C00Y	1.416(4)	C02O	C03M	1.398(5)
C00I	C00J	1.504(4)	C02O	C03O	1.507(5)
C00I	C018	1.399(4)	C02P	C035	1.380(5)
C00J	C00X	1.417(4)	C02Q	C02X	1.381(4)
C00J	C016	1.395(4)	C02R	C036	1.501(4)
C00K	C00N	1.412(4)	C02R	C03B	1.386(5)
C00K	C00Z	1.502(4)	C02R	C03I	1.405(5)

C00K	C01O	1.392(4)	C02S	C03C	1.389(4)
C00L	C01U	1.385(4)	C02T	C038	1.380(5)
C00M	C00V	1.403(4)	C02T	C03C	1.383(4)
C00M	C011	1.395(4)	C02U	C03A	1.372(5)
C00N	C013	1.406(4)	C02V	C03G	1.396(4)
C00O	C01N	1.382(4)	C02V	C040	1.505(5)
C00P	C025	1.397(4)	C033	C034	1.378(5)
C00P	C02S	1.385(4)	C034	C03G	1.377(5)
C00Q	C01E	1.404(4)	C034	C03S	1.509(4)
C00Q	C01Y	1.395(4)	C035	C03D	1.377(5)
C00R	C00S	1.388(4)	C036	C03U	1.388(4)
C00R	C01K	1.383(4)	C039	C03F	1.395(5)
C00T	C027	1.388(4)	C039	C03Z	1.394(5)
C00T	C02Y	1.510(4)	C039	C049	1.493(5)
C00U	C01C	1.387(4)	C03B	C045	1.407(5)
C00U	C02J	1.395(4)	C03B	C04C	1.501(5)
C00V	C019	1.394(4)	C03E	C03L	1.491(5)
C00X	C010	1.411(4)	C03E	C042	1.401(5)
C00Y	C01K	1.389(4)	C03F	C03N	1.485(5)
C010	C012	1.509(4)	C03F	C03R	1.397(5)
C010	C01J	1.382(4)	C03H	C03L	1.406(5)
C011	C024	1.385(4)	C03H	C03N	1.405(4)
C012	C015	1.422(4)	C03I	C03K	1.390(5)
C012	C01T	1.445(4)	C03I	C043	1.498(5)
C013	C01M	1.391(4)	C03K	C03W	1.363(6)
C013	C02D	1.517(4)	C03L	C04D	1.397(5)
C015	C02E	1.503(4)	C03M	C041	1.361(6)
C015	C02I	1.397(4)	C03N	C048	1.389(5)
C016	C017	1.396(4)	C03Q	C044	1.391(4)
C017	C01J	1.389(4)	C03R	C04B	1.409(6)
C018	C01H	1.513(4)	C03R	C04E	1.532(6)
C018	C029	1.401(4)	C03U	C044	1.373(5)
C019	C01X	1.379(4)	C03W	C045	1.373(6)
C01B	C01Q	1.406(4)	C03W	C04M	1.530(6)
C01B	C036	1.401(4)	C03Y	C041	1.385(6)
C01C	C03D	1.391(4)	C03Y	C042	1.397(5)
C01D	C01T	1.509(4)	C03Z	C046	1.362(6)
C01E	C02H	1.386(4)	C041	C04K	1.527(5)
C01F	C02C	1.392(4)	C042	C04I	1.512(6)
C01I	C01S	1.403(4)	C046	C04B	1.385(6)
C01I	C020	1.396(4)	C046	C04F	1.518(6)
C01L	C026	1.390(4)	C048	C04H	1.387(6)

C01L	C02B	1.404(4)	C04D	C04H	1.375(5)
C01M	C01V	1.390(4)			

Bond Angles for P21c_sq - Copy.

Atom	Atom	Atom	Angle/˚	Atom	Atom	Atom	Angle/˚
N008	Ni01	C00H	41.81(10)	C01V	C01M	C013	122.8(3)
N008	Ni01	C012	84.31(10)	C00O	C01N	C02Z	120.9(3)
C00H	Ni01	C012	120.88(11)	C029	C01N	C00O	117.4(3)
C01A	Ni01	N008	156.87(12)	C029	C01N	C02Z	121.7(3)
C01A	Ni01	C00H	116.44(12)	C00K	C01O	C01V	123.0(3)
C01A	Ni01	C012	118.74(12)	C022	C01P	Si06	119.0(2)
N007	Ni02	C00F	84.59(10)	C023	C01P	Si06	124.0(2)
N007	Ni02	C00W	41.77(10)	C023	C01P	C022	116.6(3)
N007	Ni02	C02A	87.92(10)	C01B	C01Q	C02F	122.5(3)
C00F	Ni02	C02A	34.56(10)	C03Q	C01Q	C01B	117.1(3)
C00W	Ni02	C00F	121.14(11)	C03Q	C01Q	C02F	120.4(3)
C00W	Ni02	C02A	129.34(10)	C02A	C01R	C02N	122.4(3)
C01G	Ni02	N007	158.41(12)	C02U	C01S	C01I	121.0(3)
C01G	Ni02	C00F	116.76(12)	C012	C01T	C01D	120.3(3)
C01G	Ni02	C00W	117.55(12)	C030	C01T	C012	119.5(3)
C01G	Ni02	C02A	111.29(12)	C030	C01T	C01D	119.9(3)
C00M	Si03	C00H	119.44(13)	C032	C01U	C00L	119.6(3)
C01I	Si03	C00H	108.13(13)	C01M	C01V	C01O	116.7(3)
C01I	Si03	C00M	107.86(12)	C01M	C01V	C03J	122.0(3)
C00E	Si04	C00H	109.77(13)	C01O	C01V	C03J	121.3(3)
C00E	Si04	C00Q	111.90(12)	C01Z	C01W	C022	120.4(3)
C00Q	Si04	C00H	110.13(12)	C019	C01X	C024	119.5(3)
C00P	Si05	C00W	110.66(13)	C02X	C01Y	C00Q	122.3(3)
C00U	Si05	C00P	111.68(12)	C01W	C01Z	C021	119.7(3)
C00U	Si05	C00W	109.46(13)	C02G	C020	C01I	120.9(3)
C00W	Si06	C01P	119.68(13)	C01Z	C021	C023	119.8(3)
C01L	Si06	C00W	108.68(13)	C01W	C022	C01P	121.1(3)
C01L	Si06	C01P	107.31(13)	C021	C023	C01P	122.3(3)
C00G	N007	Ni02	112.49(17)	C011	C024	C01X	119.9(3)
C00W	N007	Ni02	73.91(14)	C038	C025	C00P	121.5(3)
C00W	N007	C00G	126.4(2)	C031	C026	C01L	122.1(3)
C00H	N008	Ni01	73.68(14)	C02N	C027	C00T	123.1(3)
C00H	N008	C00X	126.5(2)	C01N	C029	C018	122.4(3)
C00X	N008	Ni01	112.71(17)	C00F	C02A	Ni02	60.02(15)
C01A	N009	C01B	175.4(3)	C00F	C02A	C028	121.3(3)

C01G	N00B	C03H	172.2(3)	C01R	C02A	Ni02	106.7(2)
C00G	C00C	C00N	124.1(3)	C01R	C02A	C00F	119.5(3)
C00S	C00C	C00G	117.2(3)	C01R	C02A	C028	118.8(3)
C00S	C00C	C00N	118.5(2)	C028	C02A	Ni02	108.29(19)
C00I	C00D	C014	121.3(3)	C02W	C02B	C01L	121.1(3)
C00O	C00D	C00I	119.2(3)	C032	C02C	C01F	119.7(3)
C00O	C00D	C014	119.5(2)	C02K	C02F	C01Q	120.1(3)
C00L	C00E	Si04	120.3(2)	C02K	C02F	C02V	119.7(3)
C00L	C00E	C01F	117.3(3)	C02V	C02F	C01Q	120.1(3)
C01F	C00E	Si04	122.0(2)	C03A	C02G	C020	121.0(3)
C00T	C00F	Ni02	94.85(18)	C02Q	C02H	C01E	120.5(3)
C00T	C00F	C00Y	121.7(3)	C02L	C02I	C015	123.3(3)
C00Y	C00F	Ni02	99.21(18)	C02P	C02J	C00U	121.1(3)
C02A	C00F	Ni02	85.41(18)	C02F	C02K	C04A	122.1(3)
C02A	C00F	C00T	118.1(3)	C033	C02K	C02F	119.4(3)
C02A	C00F	C00Y	119.2(2)	C033	C02K	C04A	118.5(3)
N007	C00G	C00Y	114.5(2)	C02I	C02L	C030	117.0(3)
C00C	C00G	N007	124.6(3)	C02I	C02L	C03P	122.1(3)
C00C	C00G	C00Y	120.3(3)	C030	C02L	C03P	120.9(3)
Si03	C00H	Ni01	118.27(13)	C02W	C02M	C031	120.3(3)
Si04	C00H	Ni01	102.10(13)	C01R	C02N	C03T	120.9(3)
Si04	C00H	Si03	118.00(16)	C027	C02N	C01R	117.6(3)
N008	C00H	Ni01	64.51(14)	C027	C02N	C03T	121.4(3)
N008	C00H	Si03	125.5(2)	C03E	C02O	C03O	121.2(3)
N008	C00H	Si04	113.43(18)	C03M	C02O	C03E	118.7(4)
C00D	C00I	C00J	118.9(2)	C03M	C02O	C03O	120.1(3)
C018	C00I	C00D	118.5(3)	C035	C02P	C02J	120.2(3)
C018	C00I	C00J	122.2(2)	C02H	C02Q	C02X	120.1(3)
C00X	C00J	C00I	124.1(3)	C03B	C02R	C036	119.1(3)
C016	C00J	C00I	118.2(2)	C03B	C02R	C03I	120.5(3)
C016	C00J	C00X	117.5(3)	C03I	C02R	C036	120.4(3)
C00N	C00K	C00Z	121.5(3)	C00P	C02S	C03C	122.0(3)
C01O	C00K	C00N	119.1(3)	C038	C02T	C03C	119.3(3)
C01O	C00K	C00Z	119.3(3)	C03A	C02U	C01S	120.6(3)
C01U	C00L	C00E	121.7(3)	C02F	C02V	C03G	118.7(3)
C00V	C00M	Si03	119.1(2)	C02F	C02V	C040	122.1(3)
C011	C00M	Si03	124.0(2)	C03G	C02V	C040	119.1(3)
C011	C00M	C00V	116.5(3)	C02M	C02W	C02B	119.8(3)
C00K	C00N	C00C	118.8(3)	C02Q	C02X	C01Y	119.4(3)
C013	C00N	C00C	121.9(2)	C01T	C030	C02L	123.0(3)
C013	C00N	C00K	119.0(3)	C026	C031	C02M	119.4(3)
C01N	C00O	C00D	122.7(3)	C02C	C032	C01U	120.4(3)

C025	C00P	Si05	122.4(2)	C034	C033	C02K	121.8(3)
C02S	C00P	Si05	120.6(2)	C033	C034	C03S	121.1(3)
C02S	C00P	C025	117.0(3)	C03G	C034	C033	118.1(3)
C01E	C00Q	Si04	123.2(2)	C03G	C034	C03S	120.7(4)
C01Y	C00Q	Si04	120.1(2)	C03D	C035	C02P	119.8(3)
C01Y	C00Q	C01E	116.7(3)	C01B	C036	C02R	122.0(3)
C01K	C00R	C00S	119.7(3)	C03U	C036	C01B	117.1(3)
C00R	C00S	C00C	122.5(3)	C03U	C036	C02R	120.9(3)
C00F	C00T	C02Y	121.5(3)	C02T	C038	C025	120.4(3)
C027	C00T	C00F	119.1(3)	C03F	C039	C049	121.5(4)
C027	C00T	C02Y	119.4(3)	C03Z	C039	C03F	119.1(4)
C01C	C00U	Si05	120.3(2)	C03Z	C039	C049	119.5(4)
C01C	C00U	C02J	117.4(3)	C02U	C03A	C02G	119.3(3)
C02J	C00U	Si05	122.0(2)	C02R	C03B	C045	118.4(4)
C019	C00V	C00M	121.6(3)	C02R	C03B	C04C	120.8(4)
Si05	C00W	Ni02	101.48(13)	C045	C03B	C04C	120.8(4)
Si06	C00W	Ni02	118.77(13)	C02T	C03C	C02S	119.8(3)
Si06	C00W	Si05	117.44(15)	C035	C03D	C01C	119.7(3)
N007	C00W	Ni02	64.31(14)	C02O	C03E	C03L	119.6(4)
N007	C00W	Si05	113.71(18)	C042	C03E	C02O	119.4(3)
N007	C00W	Si06	126.0(2)	C042	C03E	C03L	120.8(4)
N008	C00X	C00J	124.4(3)	C039	C03F	C03N	120.6(4)
C010	C00X	N008	114.6(2)	C039	C03F	C03R	119.8(4)
C010	C00X	C00J	120.3(3)	C03R	C03F	C03N	119.5(4)
C00G	C00Y	C00F	119.1(2)	C034	C03G	C02V	122.2(3)
C01K	C00Y	C00F	120.8(3)	N00B	C03H	C03L	118.7(3)
C01K	C00Y	C00G	120.1(3)	N00B	C03H	C03N	118.9(3)
C00X	C010	C012	119.0(2)	C03N	C03H	C03L	122.4(3)
C01J	C010	C00X	120.0(3)	C02R	C03I	C043	121.5(3)
C01J	C010	C012	120.9(3)	C03K	C03I	C02R	117.9(4)
C024	C011	C00M	122.3(3)	C03K	C03I	C043	120.6(4)
C010	C012	Ni01	99.30(18)	C03W	C03K	C03I	123.2(4)
C015	C012	Ni01	93.33(18)	C03H	C03L	C03E	122.4(3)
C015	C012	C010	122.7(3)	C04D	C03L	C03E	120.0(3)
C015	C012	C01T	117.6(3)	C04D	C03L	C03H	117.5(3)
C01T	C012	Ni01	87.14(17)	C041	C03M	C02O	122.7(4)
C01T	C012	C010	118.7(2)	C03H	C03N	C03F	121.4(3)
C00N	C013	C02D	123.1(3)	C048	C03N	C03F	121.4(3)
C01M	C013	C00N	119.5(3)	C048	C03N	C03H	117.1(4)
C01M	C013	C02D	117.4(3)	C01Q	C03Q	C044	121.0(3)
C012	C015	C02E	121.6(3)	C03F	C03R	C04B	119.0(4)
C02I	C015	C012	119.4(3)	C03F	C03R	C04E	120.5(4)

C02I	C015	C02E	118.9(3)	C04B	C03R	C04E	120.4(4)
C00J	C016	C017	122.1(3)	C044	C03U	C036	121.4(3)
C01J	C017	C016	119.4(3)	C03K	C03W	C045	118.0(4)
C00I	C018	C01H	123.3(3)	C03K	C03W	C04M	120.9(5)
C00I	C018	C029	119.7(3)	C045	C03W	C04M	121.1(5)
C029	C018	C01H	116.9(3)	C041	C03Y	C042	121.6(4)
C01X	C019	C00V	120.2(3)	C046	C03Z	C039	122.2(4)
N009	C01A	Ni01	177.0(3)	C03M	C041	C03Y	118.4(4)
N009	C01B	C01Q	118.9(2)	C03M	C041	C04K	121.1(5)
C036	C01B	N009	118.2(3)	C03Y	C041	C04K	120.5(5)
C036	C01B	C01Q	122.9(3)	C03E	C042	C04I	121.1(4)
C00U	C01C	C03D	121.8(3)	C03Y	C042	C03E	119.3(4)
C02H	C01E	C00Q	121.1(3)	C03Y	C042	C04I	119.5(4)
C02C	C01F	C00E	121.3(3)	C03U	C044	C03Q	120.3(3)
N00B	C01G	Ni02	178.8(3)	C03W	C045	C03B	122.0(4)
C01S	C01I	Si03	120.5(2)	C03Z	C046	C04B	119.0(4)
C020	C01I	Si03	122.3(2)	C03Z	C046	C04F	121.4(5)
C020	C01I	C01S	117.2(3)	C04B	C046	C04F	119.6(5)
C010	C01J	C017	120.5(3)	C04H	C048	C03N	121.7(4)
C00R	C01K	C00Y	120.0(3)	C046	C04B	C03R	120.9(5)
C026	C01L	Si06	122.7(2)	C04H	C04D	C03L	121.1(4)
C026	C01L	C02B	117.2(3)	C04D	C04H	C048	120.1(4)
C02B	C01L	Si06	120.1(2)				

Crystal data and structure refinement for $NiCOECl(DMP)_2$.

Identification code	JFig1342_1_0m_x
Empirical formula	$C_{58}H_{63}ClN_2Ni$
Formula weight	882.28
Temperature/K	100.0
Crystal system	triclinic
Space group	P-1
a/Å	15.8952(12)
b/Å	16.9832(14)
c/Å	18.9473(16)
α/°	104.762(3)
β/°	93.485(2)
γ/°	99.510(2)
Volume/Å^3	4849.6(7)
Z	4
ρ_{calc}g/cm^3	2.199
μ/mm^{-1}	5.770

F(000)	3127.0
Crystal size/mm^3	? × ? × ?
Radiation	MoKα (λ = 0.71073)
2Θ range for data collection/°	2.524 to 50.802
Index ranges	-16 ≤ h ≤ 18, -20 ≤ k ≤ 13, -22 ≤ l ≤ 22
Reflections collected	24254
Independent reflections	16479 [R_{int} = 0.0401, R_{sigma} = 0.1318]
Data/restraints/parameters	16479/0/1154
Goodness-of-fit on F^2	1.084
Final R indexes [I>=2σ (I)]	R_1 = 0.0807, wR_2 = 0.1845
Final R indexes [all data]	R_1 = 0.1544, wR_2 = 0.2234
Largest diff. peak/hole / e Å^{-3}	1.19/-1.38

Bond Lengths for JFig1342_1_0m_x.

Atom	Atom	Length/Å	Atom	Atom	Length/Å
Ni01	Cl03	2.2035(18)	C011	C018	1.399(8)
Ni01	N007	1.910(4)	C013	C01A	1.396(8)
Ni01	C00C	1.734(7)	C013	C01K	1.400(8)
Ni01	C00R	1.817(6)	C013	C025	1.495(8)
Ni02	Cl04	2.193(3)	C015	C01O	1.393(8)
Ni02	N005	1.940(5)	C015	C028	1.383(8)
Ni02	C01R	1.791(6)	C015	C02W	1.521(8)
Ni02	C1	1.415(7)	C017	C01H	1.393(8)
Ni02	Cl1	2.209(19)	C018	C01X	1.384(8)
Cl04	Cl1	0.84(5)	C018	C02K	1.520(8)
N005	C00A	1.436(7)	C019	C02E	1.405(8)
N005	C01R	1.261(7)	C019	C02O	1.497(9)
N006	C00C	1.202(7)	C01A	C020	1.488(8)
N006	C010	1.403(7)	C01B	C02P	1.526(9)
N007	C00R	1.259(7)	C01B	C02S	1.378(8)
N007	C00U	1.425(7)	C01C	C01F	1.483(8)
N008	C01M	1.411(7)	C01C	C02N	1.390(8)
N008	C1	1.517(9)	C01F	C01Y	1.411(9)
C009	C00A	1.402(7)	C01F	C023	1.400(8)
C009	C00O	1.499(7)	C01G	C01K	1.369(9)
C009	C014	1.387(8)	C01G	C01L	1.388(8)
C00A	C00B	1.387(7)	C01G	C031	1.504(8)
C00B	C00I	1.381(8)	C01H	C02Z	1.513(8)
C00B	C011	1.506(7)	C01J	C01M	1.376(8)
C00D	C019	1.385(8)	C01J	C02F	1.393(8)
C00D	C01B	1.398(8)	C01M	C02H	1.392(8)

C00D	C01I	1.507(8)	C01O	C01T	1.410(8)
C00E	C00K	1.380(8)	C01O	C02H	1.493(8)
C00E	C00Y	1.402(7)	C01R	C033	1.504(8)
C00F	C00O	1.394(8)	C01S	C01W	1.384(8)
C00F	C012	1.396(7)	C01T	C02A	1.390(9)
C00F	C01P	1.507(7)	C01T	C036	1.510(8)
C00G	C00X	1.401(8)	C01U	C028	1.384(8)
C00G	C01Z	1.369(8)	C01U	C02A	1.379(8)
C00G	C02I	1.514(8)	C01U	C02Y	1.499(9)
C00H	C00O	1.396(7)	C01V	C01X	1.372(8)
C00H	C00V	1.378(8)	C01V	C021	1.374(8)
C00H	C01E	1.512(8)	C01V	C03B	1.529(8)
C00I	C00T	1.377(8)	C01W	C01Z	1.379(8)
C00J	C011	1.394(8)	C01W	C02V	1.512(8)
C00J	C021	1.402(8)	C01Y	C02J	1.385(9)
C00J	C029	1.507(8)	C01Y	C03D	1.505(9)
C00K	C017	1.392(8)	C020	C02U	1.399(8)
C00K	C01D	1.505(7)	C022	C033	1.540(8)
C00L	C00R	1.490(8)	C022	C037	1.535(8)
C00L	C02D	1.536(8)	C023	C024	1.508(8)
C00L	C02T	1.547(8)	C023	C02Q	1.381(8)
C00M	C00Y	1.395(8)	C026	C02C	1.390(9)
C00M	C00Z	1.501(7)	C026	C02H	1.397(8)
C00M	C01H	1.399(8)	C027	C02D	1.544(9)
C00N	C00Q	1.393(8)	C027	C030	1.517(9)
C00N	C01I	1.384(8)	C02B	C033	1.559(9)
C00P	C00X	1.393(8)	C02B	C035	1.475(8)
C00P	C01S	1.391(8)	C02C	C02F	1.372(8)
C00P	C02L	1.503(8)	C02E	C02G	1.378(9)
C00Q	C016	1.383(8)	C02G	C02S	1.387(9)
C00S	C01A	1.397(8)	C02G	C039	1.523(8)
C00S	C01L	1.398(8)	C02J	C02X	1.372(9)
C00S	C032	1.519(8)	C02M	C02N	1.361(9)
C00T	C014	1.359(8)	C02M	C02U	1.395(9)
C00U	C01C	1.396(8)	C02Q	C02X	1.378(9)
C00U	C020	1.388(8)	C02R	C038	1.493(9)
C00V	C00W	1.381(8)	C02R	C03C	1.555(9)
C00W	C012	1.388(8)	C02T	C03C	1.527(9)
C00W	C01N	1.501(8)	C02X	C03F	1.508(9)
C00X	C01J	1.497(8)	C030	C038	1.312(9)
C00Y	C01Q	1.498(8)	C034	C035	1.532(9)
C00Z	C010	1.404(7)	C034	C03E	1.431(11)

C00Z	C016	1.381(8)	C037	C03A	1.486(10)
C010	C01I	1.389(7)	C03A	C03E	1.355(11)

Bond Angles for JFig1342_1_0m_x.

Atom	Atom	Atom	Angle/˚	Atom	Atom	Atom	Angle/˚
N007	Ni01	Cl03	114.16(16)	C00K	C017	C01H	122.0(5)
C00C	Ni01	Cl03	96.0(2)	C011	C018	C02K	121.1(5)
C00C	Ni01	N007	149.8(2)	C01X	C018	C011	119.5(6)
C00C	Ni01	C00R	110.7(3)	C01X	C018	C02K	119.3(5)
C00R	Ni01	Cl03	153.16(19)	C00D	C019	C02E	117.9(6)
C00R	Ni01	N007	39.4(2)	C00D	C019	C02O	123.0(5)
Cl04	Ni02	Cl1	21.9(11)	C02E	C019	C02O	119.1(5)
N005	Ni02	Cl04	111.7(2)	C00S	C01A	C02O	120.0(5)
N005	Ni02	Cl1	133.6(13)	C013	C01A	C00S	120.4(5)
C01R	Ni02	Cl04	150.7(3)	C013	C01A	C02O	119.5(6)
C01R	Ni02	N005	39.3(2)	C00D	C01B	C02P	121.4(6)
C01R	Ni02	Cl1	172.1(13)	C02S	C01B	C00D	119.4(6)
C1	Ni02	Cl04	103.1(2)	C02S	C01B	C02P	119.2(6)
C1	Ni02	N005	145.0(2)	C00U	C01C	C01F	122.5(5)
C1	Ni02	C01R	105.8(3)	C02N	C01C	C00U	117.8(6)
C1	Ni02	Cl1	81.2(13)	C02N	C01C	C01F	119.7(5)
Cl1	Cl04	Ni02	80.1(10)	C01Y	C01F	C01C	119.1(6)
C00A	N005	Ni02	155.0(4)	C023	C01F	C01C	121.5(6)
C01R	N005	Ni02	64.0(3)	C023	C01F	C01Y	119.3(6)
C01R	N005	C00A	140.7(5)	C01K	C01G	C01L	117.3(6)
C00C	N006	C010	161.1(5)	C01K	C01G	C031	121.9(6)
C00R	N007	Ni01	66.3(3)	C01L	C01G	C031	120.8(6)
C00R	N007	C00U	140.5(5)	C00M	C01H	C02Z	121.9(5)
C00U	N007	Ni01	153.0(4)	C017	C01H	C00M	118.6(6)
C01M	N008	C1	159.5(5)	C017	C01H	C02Z	119.5(5)
C00A	C009	C00O	121.6(5)	C00N	C01I	C00D	122.3(5)
C014	C009	C00A	117.7(5)	C00N	C01I	C010	117.1(5)
C014	C009	C00O	120.6(5)	C010	C01I	C00D	120.6(5)
C009	C00A	N005	117.5(4)	C01M	C01J	C00X	122.1(5)
C00B	C00A	N005	120.8(5)	C01M	C01J	C02F	116.7(6)
C00B	C00A	C009	121.6(5)	C02F	C01J	C00X	121.2(6)
C00A	C00B	C011	123.9(5)	C01G	C01K	C013	123.9(5)
C00I	C00B	C00A	117.5(5)	C01G	C01L	C00S	121.7(6)
C00I	C00B	C011	118.6(5)	C01J	C01M	N008	119.7(5)
N006	C00C	Ni01	174.0(5)	C01J	C01M	C02H	124.0(5)

C019	C00D	C01B	120.9(5)	C02H	C01M	N008	116.4(6)
C019	C00D	C01I	120.8(5)	C015	C01O	C01T	120.4(6)
C01B	C00D	C01I	118.2(5)	C015	C01O	C02H	119.1(5)
C00K	C00E	C00Y	122.2(6)	C01T	C01O	C02H	120.3(5)
C00O	C00F	C012	118.8(5)	N005	C01R	Ni02	76.8(4)
C00O	C00F	C01P	121.3(5)	N005	C01R	C033	141.3(6)
C012	C00F	C01P	119.9(5)	C033	C01R	Ni02	142.0(5)
C00X	C00G	C02I	120.4(6)	C01W	C01S	C00P	121.5(6)
C01Z	C00G	C00X	118.8(5)	C01O	C01T	C036	120.5(6)
C01Z	C00G	C02I	120.8(5)	C02A	C01T	C01O	118.0(6)
C00O	C00H	C01E	121.0(5)	C02A	C01T	C036	121.5(6)
C00V	C00H	C00O	118.6(5)	C028	C01U	C02Y	122.2(6)
C00V	C00H	C01E	120.5(5)	C02A	C01U	C028	117.5(6)
C00T	C00I	C00B	122.3(5)	C02A	C01U	C02Y	120.3(6)
C011	C00J	C021	118.4(5)	C01X	C01V	C021	118.8(5)
C011	C00J	C029	120.9(5)	C01X	C01V	C03B	119.9(6)
C021	C00J	C029	120.7(5)	C021	C01V	C03B	121.2(6)
C00E	C00K	C017	118.0(5)	C01S	C01W	C02V	121.0(5)
C00E	C00K	C01D	120.4(6)	C01Z	C01W	C01S	118.2(6)
C017	C00K	C01D	121.6(5)	C01Z	C01W	C02V	120.8(5)
C00R	C00L	C02D	107.3(5)	C01V	C01X	C018	121.4(6)
C00R	C00L	C02T	109.4(5)	C01F	C01Y	C03D	119.7(6)
C02D	C00L	C02T	114.2(5)	C02J	C01Y	C01F	118.6(6)
C00Y	C00M	C00Z	120.0(5)	C02J	C01Y	C03D	121.7(6)
C00Y	C00M	C01H	120.8(5)	C00G	C01Z	C01W	122.5(5)
C01H	C00M	C00Z	119.1(5)	C00U	C020	C01A	122.9(5)
C01I	C00N	C00Q	121.2(5)	C00U	C020	C02U	116.8(6)
C00F	C00O	C009	118.8(5)	C02U	C020	C01A	120.3(5)
C00F	C00O	C00H	120.5(5)	C01V	C021	C00J	121.8(6)
C00H	C00O	C009	120.6(5)	C037	C022	C033	114.4(5)
C00X	C00P	C02L	120.9(6)	C01F	C023	C024	121.3(6)
C01S	C00P	C00X	118.9(5)	C02Q	C023	C01F	118.9(6)
C01S	C00P	C02L	120.2(6)	C02Q	C023	C024	119.8(6)
C016	C00Q	C00N	119.5(5)	C02C	C026	C02H	120.2(6)
N007	C00R	Ni01	74.3(4)	C030	C027	C02D	114.6(5)
N007	C00R	C00L	139.7(5)	C015	C028	C01U	122.7(6)
C00L	C00R	Ni01	146.0(4)	C01U	C02A	C01T	122.7(6)
C01A	C00S	C01L	119.1(5)	C035	C02B	C033	116.3(5)
C01A	C00S	C032	121.1(6)	C02F	C02C	C026	120.1(6)
C01L	C00S	C032	119.8(6)	C00L	C02D	C027	117.4(5)
C014	C00T	C00I	119.0(6)	C02G	C02E	C019	122.0(6)
C01C	C00U	N007	117.5(5)	C02C	C02F	C01J	121.7(6)

C020	C00U	N007	119.3(5)	C02E	C02G	C02S	118.5(6)
C020	C00U	C01C	123.1(5)	C02E	C02G	C039	120.7(6)
C00H	C00V	C00W	122.8(5)	C02S	C02G	C039	120.8(6)
C00V	C00W	C012	117.8(5)	C01M	C02H	C01O	120.4(5)
C00V	C00W	C01N	121.3(5)	C01M	C02H	C026	117.2(6)
C012	C00W	C01N	120.9(6)	C026	C02H	C01O	122.4(5)
C00G	C00X	C01J	120.5(5)	C02X	C02J	C01Y	122.9(6)
C00P	C00X	C00G	120.1(6)	C02N	C02M	C02U	120.3(6)
C00P	C00X	C01J	119.4(5)	C02M	C02N	C01C	121.0(6)
C00E	C00Y	C01Q	119.5(5)	C02X	C02Q	C023	122.8(6)
C00M	C00Y	C00E	118.4(5)	C038	C02R	C03C	111.6(6)
C00M	C00Y	C01Q	122.1(5)	C01B	C02S	C02G	121.3(6)
C010	C00Z	C00M	122.1(5)	C03C	C02T	C00L	114.1(5)
C016	C00Z	C00M	121.3(5)	C02M	C02U	C020	120.9(6)
C016	C00Z	C010	116.6(5)	C02J	C02X	C02Q	117.4(6)
N006	C010	C00Z	118.1(5)	C02J	C02X	C03F	122.0(7)
C01I	C010	N006	118.2(5)	C02Q	C02X	C03F	120.6(7)
C01I	C010	C00Z	123.5(5)	C038	C030	C027	123.3(6)
C00J	C011	C00B	120.9(5)	C01R	C033	C022	108.0(5)
C00J	C011	C018	119.8(5)	C01R	C033	C02B	108.3(5)
C018	C011	C00B	119.2(5)	C022	C033	C02B	112.9(5)
C00W	C012	C00F	121.5(6)	C03E	C034	C035	112.5(6)
C01A	C013	C01K	117.5(6)	C02B	C035	C034	116.8(5)
C01A	C013	C025	121.5(5)	C03A	C037	C022	118.9(6)
C01K	C013	C025	121.0(5)	C030	C038	C02R	123.9(6)
C00T	C014	C009	121.9(5)	C03E	C03A	C037	121.9(8)
C01O	C015	C02W	121.3(6)	C02T	C03C	C02R	114.0(5)
C028	C015	C01O	118.7(6)	C03A	C03E	C034	126.8(9)
C028	C015	C02W	120.0(5)	Ni02	C1	N008	172.8(4)
C00Z	C016	C00Q	121.8(5)	Cl04	Cl1	Ni02	78.0(19)

Crystal data and structure refinement for $Ni(SiCl_3)_2(DMP)_3OEt_2$.

Identification code	JFig1350
Empirical formula	$C_{79}H_{85}Cl_6N_3ONiS_{i2}$
Formula weight	1420.12
Temperature/K	100.0
Crystal system	monoclinic
Space group	$P2_1/n$
a/Å	13.006(14)
b/Å	31.12(3)
c/Å	18.843(19)

α/°	90
β/°	99.520(10)
γ/°	90
Volume/Å^3	7521(14)
Z	4
ρ_{calc}g/cm^3	1.178
μ/mm^{-1}	0.546
F(000)	2644.0
Crystal size/mm^3	? × ? × ?
Radiation	MoKα (λ = 0.71073)
2Θ range for data collection/°	2.552 to 50.79
Index ranges	-6 ≤ h ≤ 15, -34 ≤ k ≤ 24, -22 ≤ l ≤ 13
Reflections collected	15490
Independent reflections	11293 [R_{int} = 0.0431, R_{sigma} = 0.0888]
Data/restraints/parameters	11293/0/829
Goodness-of-fit on F^2	1.265
Final R indexes [I>=2σ (I)]	R_1 = 0.0760, wR_2 = 0.2032
Final R indexes [all data]	R_1 = 0.1153, wR_2 = 0.2296
Largest diff. peak/hole / e Å^{-3}	0.65/-0.74

Bond Lengths for JFig1350.

Atom	Atom	Length/Å	Atom	Atom	Length/Å
Ni01	Si06	2.221(2)	C00V	C01S	1.412(9)
Ni01	Si09	2.231(2)	C00W	C01X	1.426(9)
Ni01	C00D	1.808(6)	C00W	C01Y	1.517(10)
Ni01	C00F	1.852(7)	C00X	C01E	1.420(9)
Ni01	C00J	1.853(7)	C00X	C01L	1.507(10)
Cl02	Si06	2.061(3)	C00Y	C01Q	1.403(11)
Cl03	Si06	2.071(3)	C00Z	C013	1.397(9)
Cl04	Si06	2.061(3)	C00Z	C01N	1.386(9)
Cl05	Si09	2.062(3)	C00Z	C02E	1.530(10)
Cl07	Si09	2.076(3)	C010	C01G	1.389(9)
Cl08	Si09	2.050(3)	C012	C014	1.391(9)
N00A	C00F	1.159(7)	C013	C014	1.393(9)
N00A	C00I	1.409(7)	C013	C01K	1.475(9)
N00B	C00D	1.172(7)	C014	C021	1.529(9)
N00B	C00E	1.407(7)	C015	C017	1.392(9)
N00C	C00J	1.164(8)	C015	C018	1.388(10)
N00C	C016	1.409(8)	C015	C020	1.543(9)
C00E	C00H	1.394(8)	C016	C01K	1.384(10)
C00E	C00L	1.387(8)	C016	C01M	1.409(9)

C00G	C00H	1.501(8)	C019	C01J	1.405(9)
C00G	C00O	1.394(9)	C019	C025	1.488(11)
C00G	C00X	1.395(9)	C01B	C01M	1.471(10)
C00H	C00R	1.416(8)	C01B	C01U	1.409(10)
C00I	C00N	1.404(9)	C01B	C01V	1.390(10)
C00I	C00V	1.389(9)	C01C	C01J	1.408(11)
C00K	C00L	1.498(8)	C01C	C01X	1.374(11)
C00K	C00W	1.384(9)	C01C	C01Z	1.529(9)
C00K	C019	1.399(9)	C01D	C01F	1.375(10)
C00L	C01G	1.401(8)	C01D	C01I	1.382(9)
C00M	C00N	1.475(10)	C01E	C01Q	1.386(11)
C00M	C00U	1.414(9)	C01F	C024	1.545(9)
C00M	C01F	1.429(9)	C01H	C01I	1.412(9)
C00N	C01O	1.401(9)	C01I	C022	1.511(10)
C00O	C00Y	1.400(9)	C01K	C02C	1.409(10)
C00O	C01P	1.509(10)	C01M	C02D	1.415(10)
C00P	C011	1.398(9)	C01O	C01R	1.379(11)
C00P	C017	1.396(9)	C01Q	C02A	1.557(10)
C00P	C01T	1.528(9)	C01R	C01S	1.420(10)
C00Q	C011	1.398(8)	C01U	C023	1.382(11)
C00Q	C018	1.389(9)	C01U	C028	1.495(10)
C00Q	C01W	1.523(9)	C01V	C026	1.379(11)
C00R	C010	1.412(9)	C01V	C02B	1.527(11)
C00S	C012	1.396(9)	C023	C029	1.411(11)
C00S	C01N	1.387(10)	C026	C029	1.419(12)
C00S	C027	1.520(10)	C029	C02G	1.498(12)
O00T	C02H	1.423(11)	C02C	C02F	1.400(11)
O00T	C02J	1.412(13)	C02D	C02F	1.389(13)
C00U	C01A	1.518(9)	C02H	C02I	1.500(17)
C00U	C01H	1.388(9)	C02J	C02K	1.610(15)
C00V	C011	1.484(9)			

Bond Angles for JFig1350.

Atom	Atom	Atom	Angle/˚	Atom	Atom	Atom	Angle/˚
Si06	Ni01	Si09	173.78(7)	C00G	C00X	C01L	122.3(6)
C00D	Ni01	Si06	87.7(2)	C01E	C00X	C01L	119.0(6)
C00D	Ni01	Si09	87.2(2)	C00O	C00Y	C01Q	119.8(7)
C00D	Ni01	C00F	124.3(3)	C013	C00Z	C02E	120.0(6)
C00D	Ni01	C00J	121.6(3)	C01N	C00Z	C013	119.6(6)
C00F	Ni01	Si06	92.2(2)	C01N	C00Z	C02E	120.4(6)

C00F	Ni01	Si09	93.6(2)	C01G	C010	C00R	121.0(5)
C00F	Ni01	C00J	114.1(2)	C00P	C011	C00Q	119.6(6)
C00J	Ni01	Si06	90.3(2)	C00P	C011	C00V	119.3(5)
C00J	Ni01	Si09	89.4(2)	C00Q	C011	C00V	121.0(6)
Cl02	Si06	Ni01	114.84(11)	C014	C012	C00S	120.3(7)
Cl02	Si06	Cl03	103.45(10)	C00Z	C013	C01K	119.0(6)
Cl03	Si06	Ni01	114.72(10)	C014	C013	C00Z	120.3(6)
Cl04	Si06	Ni01	115.07(10)	C014	C013	C01K	120.6(6)
Cl04	Si06	Cl02	103.87(10)	C012	C014	C013	119.5(6)
Cl04	Si06	Cl03	103.37(12)	C012	C014	C021	120.8(6)
Cl05	Si09	Ni01	112.37(11)	C013	C014	C021	119.6(6)
Cl05	Si09	Cl07	102.89(10)	C017	C015	C020	118.7(7)
Cl07	Si09	Ni01	116.92(11)	C018	C015	C017	119.2(6)
Cl08	Si09	Ni01	115.81(10)	C018	C015	C020	122.1(6)
Cl08	Si09	Cl05	104.08(10)	N00C	C016	C01M	116.9(6)
Cl08	Si09	Cl07	103.13(11)	C01K	C016	N00C	119.6(6)
C00F	N00A	C00I	176.7(6)	C01K	C016	C01M	123.5(6)
C00D	N00B	C00E	177.8(6)	C015	C017	C00P	120.5(7)
C00J	N00C	C016	177.4(6)	C015	C018	C00Q	121.0(6)
N00B	C00D	Ni01	178.8(5)	C00K	C019	C01J	118.6(7)
C00H	C00E	N00B	117.2(5)	C00K	C019	C025	121.1(6)
C00L	C00E	N00B	119.0(5)	C01J	C019	C025	120.3(7)
C00L	C00E	C00H	123.8(5)	C01U	C01B	C01M	118.7(7)
N00A	C00F	Ni01	178.1(5)	C01V	C01B	C01M	119.8(7)
C00O	C00G	C00H	119.6(6)	C01V	C01B	C01U	121.3(7)
C00O	C00G	C00X	121.2(6)	C01J	C01C	C01Z	119.4(7)
C00X	C00G	C00H	119.2(6)	C01X	C01C	C01J	120.4(6)
C00E	C00H	C00G	124.8(5)	C01X	C01C	C01Z	120.1(7)
C00E	C00H	C00R	117.6(5)	C01F	C01D	C01I	121.2(7)
C00R	C00H	C00G	117.5(5)	C01Q	C01E	C00X	120.2(7)
C00N	C00I	N00A	118.2(6)	C00M	C01F	C024	119.5(7)
C00V	C00I	N00A	118.6(5)	C01D	C01F	C00M	120.0(6)
C00V	C00I	C00N	123.2(6)	C01D	C01F	C024	120.5(6)
N00C	C00J	Ni01	179.4(6)	C010	C01G	C00L	120.3(6)
C00W	C00K	C00L	118.9(6)	C00U	C01H	C01I	120.3(6)
C00W	C00K	C019	121.4(6)	C01D	C01I	C01H	119.7(7)
C019	C00K	C00L	119.7(6)	C01D	C01I	C022	120.1(7)
C00E	C00L	C00K	123.3(5)	C01H	C01I	C022	120.2(7)
C00E	C00L	C01G	118.0(5)	C019	C01J	C01C	120.3(7)
C01G	C00L	C00K	118.7(5)	C016	C01K	C013	124.0(6)
C00U	C00M	C00N	120.4(6)	C016	C01K	C02C	118.5(7)
C00U	C00M	C01F	118.8(7)	C02C	C01K	C013	117.5(7)

C01F	C00M	C00N	120.7(6)	C016	C01M	C01B	124.7(6)
C00I	C00N	C00M	124.0(6)	C016	C01M	C02D	117.4(8)
C01O	C00N	C00I	117.1(7)	C02D	C01M	C01B	117.9(6)
C01O	C00N	C00M	118.9(6)	C00Z	C01N	C00S	120.5(6)
C00G	C00O	C00Y	119.7(7)	C01R	C01O	C00N	121.7(7)
C00G	C00O	C01P	121.3(6)	C00Y	C01Q	C02A	120.3(8)
C00Y	C00O	C01P	119.0(6)	C01E	C01Q	C00Y	120.4(6)
C011	C00P	C01T	122.6(6)	C01E	C01Q	C02A	119.3(8)
C017	C00P	C011	119.9(6)	C01O	C01R	C01S	120.2(6)
C017	C00P	C01T	117.5(6)	C00V	C01S	C01R	119.2(7)
C011	C00Q	C01W	120.7(6)	C01B	C01U	C028	121.5(7)
C018	C00Q	C011	119.8(6)	C023	C01U	C01B	119.2(7)
C018	C00Q	C01W	119.5(6)	C023	C01U	C028	119.3(7)
C010	C00R	C00H	119.3(6)	C01B	C01V	C02B	121.5(8)
C012	C00S	C027	120.0(7)	C026	C01V	C01B	119.3(7)
C01N	C00S	C012	119.7(6)	C026	C01V	C02B	119.2(8)
C01N	C00S	C027	120.2(6)	C01C	C01X	C00W	119.6(7)
C02J	O00T	C02H	113.2(10)	C01U	C023	C029	120.6(8)
C00M	C00U	C01A	119.9(6)	C01V	C026	C029	120.9(8)
C01H	C00U	C00M	119.9(6)	C023	C029	C026	118.7(8)
C01H	C00U	C01A	120.2(6)	C023	C029	C02G	122.1(8)
C00I	C00V	C011	124.1(5)	C026	C029	C02G	119.2(8)
C00I	C00V	C01S	118.4(6)	C02F	C02C	C01K	118.7(9)
C01S	C00V	C011	117.5(6)	C02F	C02D	C01M	119.3(7)
C00K	C00W	C01X	119.5(7)	C02D	C02F	C02C	122.6(8)
C00K	C00W	C01Y	121.7(6)	O00T	C02H	C02I	107.2(10)
C01X	C00W	C01Y	118.8(7)	O00T	C02J	C02K	104.3(10)
C00G	C00X	C01E	118.7(6)				

References

1. Kumar, K. A.; Sreelekha, T. S.; Shivakumara, K. N.; Prakasha, K. C.; Gowda, D. C., Zinc-catalyzed reduction of imines by triethylsilane. *Synth. Commun.* **2009,** *39* (8), 1332-1341.

2. Bhunia, M.; Hota, P. K.; Vijaykumar, G.; Adhikari, D.; Mandal, S. K., A Highly Efficient Base-Metal Catalyst: Chemoselective Reduction of Imines to Amines Using An Abnormal-NHC-Fe(0) Complex. *Organometallics* **2016**, Ahead of Print.

3. Castro, L. C. M.; Sortais, J.-B.; Darcel, C., NHC-carbene cyclopentadienyl iron based catalyst for a general and efficient hydrosilylation of imines. *Chem Commun (Camb)* **2012,** *48* (1), 151-3.

4. Li, B.; Bheeter, C. B.; Darcel, C.; Dixneuf, P. H., Sequential catalysis for the production of sterically hindered amines: Ru(II)-catalyzed C-H bond activation and hydrosilylation of imines. *ACS Catalysis* **2011,** *1* (10), 1221-1224.

5. Li, B.; Sortais, J.-B.; Darcel, C.; Dixneuf, P. H., Amine Synthesis through Mild Catalytic Hydrosilylation of Imines using Polymethylhydroxysiloxane and [RuCl2(arene)]2 Catalysts. *ChemSusChem* **2012,** *5* (2), 396-399.

6. Li, B.; Bheeter, C. B.; Darcel, C.; Dixneuf, P. H., Sequential Ruthenium(II)-Acetate Catalyzed C-H Bond Diarylation in NMP or Water and Hydrosilylation of Imines. *Topics in Catalysis* **2014,** *57* (10-13), 833-842.

7. Nishibayashi, Y.; Takei, I.; Uemura, S.; Hidai, M., Ruthenium-Catalyzed Asymmetric Hydrosilylation of Ketones and Imine. *Organometallics* **1998,** *17* (16), 3420-3422.

8. Zhorov, E. Y.; Pavlov, V. A.; Fedotova, O. A.; Shvedov, V. I.; Mistryukov, E. A.; Platonov, D. N.; Gorshkova, L. S.; Klabunovskii, E. I., Enantioselective metal-complex catalysis. 7. Asymmetric hydrosilylation of imines and oximes on the rhodium [Rh(COD)Cl]2/(S)-Phephos catalyst. *Izv. Akad. Nauk SSSR, Ser. Khim.* **1991,** (4), 865-8.

9. Langlois, N.; Dang, T. P.; Kagan, H. B., Asymmetric synthesis of amines by hydrosilylation of imines catalyzed by a chiral complex of rhodium. *Tetrahedron Lett.* **1973,** (49), 4865-8.

10. Corre, Y.; Iali, W.; Hamdaoui, M.; Trivelli, X.; Djukic, J. P.; Agbossou-Niedercorn, F.; Michon, C., Efficient hydrosilylation of imines using catalysts based on iridium(iii) metallacycles. *Catalysis Science & Technology* **2015**.

11. Takei, I.; Nishibayashi, Y.; Arikawa, Y.; Uemura, S.; Hidai, M., Iridium-Catalyzed Asymmetric Hydrosilylation of Imines Using Chiral Oxazolinyl-Phosphine Ligands. *Organometallics* **1999,** *18* (11), 2271-2274.

12. Field, L. D.; Messerle, B. A.; Rumble, S. L., Iridium(I)-catalyzed tandem hydrosilylation-protodesilylation of imines. *Eur. J. Org. Chem.* **2005,** (14), 2881-2883.

13. Mirza-Aghayan, M.; Boukherroub, R.; Rahimifard, M., Palladium(II) acetate-catalyzed reduction of imines to the corresponding amines by triethylsilane. *Appl. Organomet. Chem.* **2013,** *27* (3), 174-176.

14. Vetter, A. H.; Berkessel, A., Nickel complex catalyzed reduction of imines. *Synthesis* **1995,** (4), 419-22.

15. Bheeter, L. P.; Henrion, M.; Chetcuti, M. J.; Darcel, C.; Ritleng, V.; Sortais, J.-B., Cyclopentadienyl N-heterocyclic carbene-nickel complexes as efficient pre-catalysts for the hydrosilylation of imines. *Catal. Sci. Technol.* **2013,** *3* (12), 3111-3116.

16. Xiao, M.; Hochberg, A. K. Synthesis of aminosilane precursors for CVD silicon carbonitride dielectric films. US20060258173A1, 2006.

17. Xiao, M.; MacDonald, M. R.; Ho, R.; Lei, X. Organoaminosilanes and methods for making same. EP2913334A1, 2015.

18. Fox, B. J.; Millard, M. D.; DiPasquale, A. G.; Rheingold, A. L.; Figueroa, J. S., Thallium(I) as a Coordination Site Protection Agent: Preparation of an Isolable Zero-Valent Nickel Tris-Isocyanide. *Angew. Chem., Int. Ed.* **2009,** *48* (19), 3473-3477, S3473/1-S3473/19.

19. Labios, L. A.; Millard, M. D.; Rheingold, A. L.; Figueroa, J. S., Bond Activation, Substrate Addition and Catalysis by an Isolable Two-Coordinate Pd(0) Bis-Isocyanide Monomer. *Journal of the American Chemical Society* **2009,** *131* (32), 11318-11319.

20. Carpenter, A. E.; Wen, I.; Moore, C. E.; Rheingold, A. L.; Figueroa, J. S., [1,1-Co2(CO)6(CNAr Mes 2)2]: A Structural Mimic of the Elusive D2d Isomer of [Co2(CO)8]. *Chemistry – A European Journal* **2013,** *19* (32), 10452-10457.

21. Mokhtarzadeh, C. C.; Margulieux, G. W.; Carpenter, A. E.; Weidemann, N.; Moore, C. E.; Rheingold, A. L.; Figueroa, J. S., Synthesis and Protonation of an Encumbered Iron Tetraisocyanide Dianion. *Inorganic Chemistry* **2015,** *54* (11), 5579-5587.

22. Margulieux, G. W.; Weidemann, N.; Lacy, D. C.; Moore, C. E.; Rheingold, A. L.; Figueroa, J. S., Isocyano Analogues of [Co(CO)4]n: A Tetraisocyanide of Cobalt Isolated in Three States of Charge. *Journal of the American Chemical Society* **2010,** *132* (14), 5033-5035.

23. Jonas, K.; Wilke, G., Hydrogen bonds in a Ni-Ni system. *Angew. Chem., Int. Ed. Engl.* **1970,** *9* (4), 312-13.

24. Carpenter, A. E.; Rheingold, A. L.; Figueroa, J. S., A Well-Defined Isocyano Analogue of HCo(CO)4. 1: Synthesis, Decomposition, and Catalytic 1,1-Hydrogenation of Isocyanides. *Organometallics* **2016,** *35* (14), 2309-2318.

25. Ogoshi, S.; Ikeda, H.; Kurosawa, H., Nickel-catalyzed [2+2+2] cycloaddition of two alkynes and an imine. *Pure Appl. Chem.* **2008,** *80* (5), 1115-1125.

26. Iluc, V. M.; Hillhouse, G. L., Arrested 1,2-Hydrogen Migration from Silicon to Nickel upon Oxidation of a Three-Coordinate Ni(I) Silyl Complex. *J. Am. Chem. Soc.* **2010,** *132* (34), 11890-11892.

27. Beck, R.; Johnson, S. A., Structural Similarities in Dinuclear, Tetranuclear, and Pentanuclear Nickel Silyl and Silylene Complexes Obtained via Si-H and Si-C Activation. *Organometallics* **2012,** *31* (9), 3599-3609.

28. Corey, J. Y., Reactions of Hydrosilanes with Transition Metal Complexes. *Chem. Rev. (Washington, DC, U. S.)* **2016,** *116* (19), 11291-11435.

29. Zell, T.; Schaub, T.; Radacki, K.; Radius, U., Si-H Activation of hydrosilanes leading to hydrido silyl and bis(silyl) nickel complexes. *Dalton Trans.* **2011,** *40* (9), 1852-1854.

30. MacMillan, S. N.; Hill Harman, W.; Peters, J. C., Facile Si-H bond activation and hydrosilylation catalysis mediated by a nickel-borane complex. *Chem. Sci.* **2014,** *5* (2), 590-597.

31. Chalk, A. J.; Harrod, J. F., Homogeneous catalysis. II. The mechanism of the hydrosilation of olefins catalyzed by Group VIII metal complexes. *J. Am. Chem. Soc.* **1965,** *87* (1), 16-21.

32. Aitken, C.; Harrod, J. F.; Samuel, E., Polymerization of primary silanes to linear polysilanes catalyzed by titanocene derivatives. *J. Organomet. Chem.* **1985,** *279* (1-2), C11-C13.

33. Smith, E. E.; Du, G.-D.; Fanwick, P. E.; Abu-Omar, M. M., Dehydrocoupling of Organosilanes with a Dinuclear Nickel Hydride Catalyst and Isolation of a Nickel Silyl Complex. *Organometallics* **2010,** *29* (23), 6527-6533.

34. Tanabe, M.; Takahashi, A.; Fukuta, T.; Osakada, K., Nickel-Catalyzed Cyclopolymerization of Hexyl- and Phenylsilanes. *Organometallics* **2013,** *32* (4), 1037-1043.

35. Schmidt, D.; Zell, T.; Schaub, T.; Radius, U., Si-H bond activation at {(NHC)2Ni0} leading to hydrido silyl and bis(silyl) complexes: a versatile tool for catalytic Si-H/D exchange, acceptorless dehydrogenative coupling of hydrosilanes, and hydrogenation of disilanes to hydrosilanes. *Dalton Trans* **2014,** *43* (28), 10816-27.

36. Emerich, B. M.; Moore, C. E.; Fox, B. J.; Rheingold, A. L.; Figueroa, J. S., Protecting-Group-Free Access to a Three-Coordinate Nickel(0) Tris-isocyanide. *Organometallics* **2011,** *30* (9), 2598-2608.

37. Yempally, V.; Zhu, L.; Isrow, D.; Captain, B., Synthesis and characterization of bimetallic nickel and cobalt carbonyl complexes containing stannyl groups. *J. Cluster Sci.* **2010,** *21* (3), 417-426.